Bull Volcanol (2007) 69:903–926
DOI 10.1007/s00445-007-0117-6

RESEARCH ARTICLE

Contrasting grain size and componentry in complex proximal deposits of the 1886 Tarawera basaltic Plinian eruption

R. J. Carey · B. F. Houghton · J. E. Sable · C. J. N. Wilson

Received: 5 August 2004 / Accepted: 3 January 2007 / Published online: 1 March 2007

Abstract The 1886 Plinian eruption of Tarawera, New Zealand, is a unique basaltic fissure-fed eruption with exceptionally well preserved fall deposits to within 200 meters of the source vents. These proximal deposits form a series of spatter/cinder half-cones along the northeastern 8-km-long segment of the 1886 fissure. Here we examine these deposits using grain size and clast componentry techniques. We contrast the products of the phreatomagmatic (phases I and III) and Plinian (Phase II) stages of the eruption and examine deposit variability as a function of contrasting eruptive intensity within the climactic phase (II) of the eruption. The opening phreatomagmatic phase I of the eruption involved gas-rich magma interacting with water and fragmenting at least 300 meters below the surface. The deposits of the climactic phase that followed have relatively uniform grain size but marked contrasts in the relative abundance of juvenile and wall rock (lithic) clasts. Deposits linked to vents associated with the high Plinian plume are more uniform than those characterized by a weaker cone-forming eruption style. During the third, and closing, phase of the eruption, magma withdrawal accompanied the onset of decoupling of the exsolved gas phase, leading to fragmentation at increasingly greater depths and significant wall rock collapse into the erupting vents. Variability in eruptive style during phase II along the fissure appears to be a function of shallow seated controls, in particular the variable extent of incorporation of lithic wall rock into the erupting jet, as a consequence of vent wall collapse. Widely dispersed beds centralized around Plinian sources along the fissure have very low lithic content; cone-forming beds at other craters that contain very high lithic contents. This incorporation led to a significant reduction of the velocity and stability of the jet at these latter steep-walled craters, and induced episodicity in the form of vent-clearing explosions. The result is a large reduction of the physical and thermal ability of these vents to contribute to a stable high eruptive plume. Instead large volumes of ejecta were sedimented prematurely from shallow heights at rates an order of magnitude greater than for historical Strombolian, Hawaiian and subPlinian eruptions. This study illustrates that sustained powerful Plinian eruptions can be accompanied by heterogeneities and instabilities of the eruptive jet. At Tarawera, the record of complex proximal transport and deposition processes in the eruptive jet cannot be inferred from the eruption products at distances greater than 400 m from the eruptive fissure. We suggest that study of ultraproximal deposits, as seen at Mt Tarawera, provides the only opportunity to document the complex, dynamic behavior of the jet region of Plinian eruptions.

Keywords Plinian eruption · Tarawera 1886 · Basaltic Plinian · Fall deposit

Editorial responsibility: R Cioni

R. J. Carey (✉) · B. F. Houghton · J. E. Sable
Department of Geology and Geophysics, SOEST,
University of Hawaii,
1680 East-West Road,
Honolulu, HI 96822, USA
e-mail: beccarey@soest.hawaii.edu

C. J. N. Wilson
School of Geography, Geology and Environmental Science,
University of Auckland,
P.O. Box 92019, Auckland 1142, New Zealand

Introduction

The 1886 eruption of Tarawera was one of three events featured in two landmark papers which recognized that

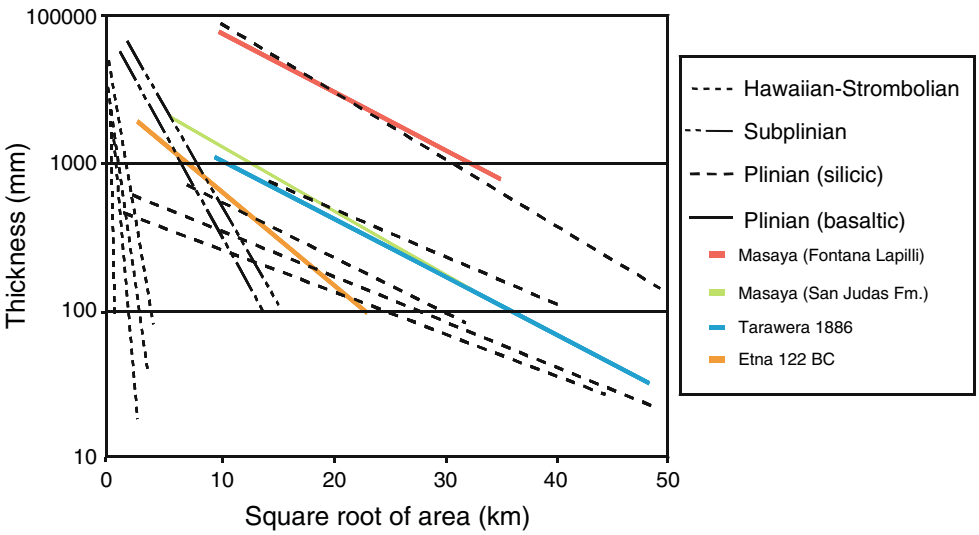

Fig. 1 Plot of thickness versus square root of area for four basaltic Plinian deposits (*bold colored lines*), after Pyle (1989). For comparison, data is shown for four historical Hawaiian-Strombolian, two subPlinian and five silicic Plinian deposits

basaltic magmas can erupt in Plinian fashion (Walker et al. 1984; Williams 1983). The 1886 eruption (Fig. 1), is the most recent of only four documented cases of basaltic Plinian events (Williams 1983; Walker et al. 1984; Coltelli et al. 1995). Subaerial basaltic volcanism is more typically characterized by effusive or mildly explosive eruptions, ranging from Hawaiian fire fountaining to discrete Strombolian explosions, and explosive phases generally form locally dispersed cones of scoria and ash, e.g. eruptions at Stromboli, Etna and Kilauea (Walker and Croasdale 1972;

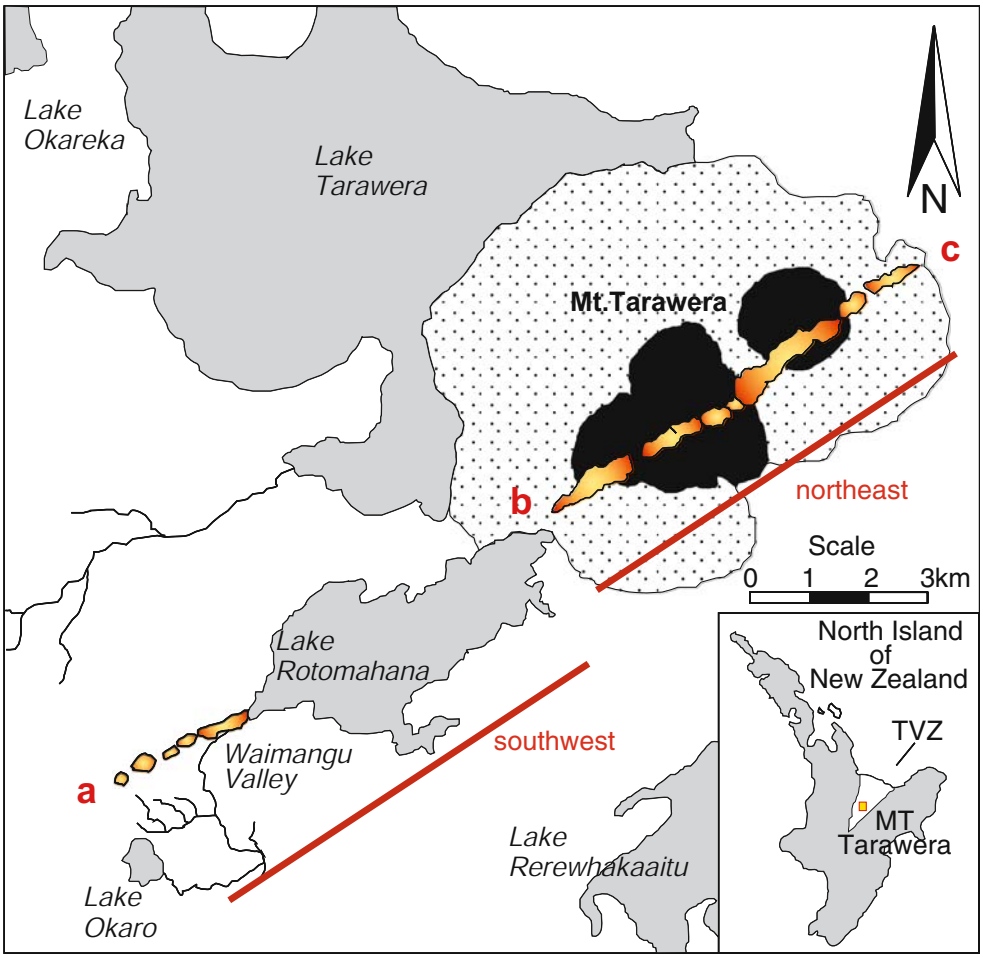

Fig. 2 Location map. The 1886 eruption fissure (**a**–**c**) extends 17 km from the Waimangu geothermal field to Mt Tarawera. The 1314 A.D. Kaharoa lava domes defining the pre-eruptive Mt Tarawera and the northeastern portion of the fissure, are shown *in black*. Older rhyolitic domes and pyroclastics from the 18,000, 15,000 and 11,000 ^{14}C yr B.P. eruption episodes are stippled. Modern Lake Rotomahana occupies at least five coalesced craters from the 1886 eruption. This paper focuses on the northeast portion of the 1886 fissure (**b**, **c**)

Wilson and Head 1981; Parfitt and Wilson 1995; Jaupart 1996). Tarawera is the only basaltic Plinian eruption for which there are detailed written accounts from eyewitnesses.

Okataina Volcanic Centre and Tarawera volcano

The Okataina Volcanic Centre is the most recently active of eight major silicic eruptive centers within Taupo Volcanic Zone (TVZ) in northern New Zealand (Fig. 2) (Houghton et al. 1995; Wilson et al. 1995). Two vent lineations have formed above major fracture zones that cross the ~62 ka Okataina caldera, parallel to the structural fabric of TVZ. The Tarawera lineament (a–b in Fig. 2) was the locus of rhyolitic eruptions at 18,000, 15,000, 11,000 and 700 (1314 AD) ^{14}C years ago as well as the site of vents of the 1886 eruption (Cole 1970; Nairn and Cole 1981). Small volumes of basalt were erupted during two of the four rhyolitic eruptions (Leonard et al. 2002). During the 1314 AD Kaharoa eruption four summit lava domes (Fig. 2) were extruded and voluminous block and ash flows were generated by the collapse from the margins of the growing domes (Nairn et al. 2001). These domes define Mt Tarawera and establish the surface 'architecture' of the vent region for the 1886 eruption (Fig. 2) The Kaharoa domes and pyroclastic deposits represent a major, easily identified source of wall-rock lithic clasts in the 1886 deposits, which played a key role during the eruption.

The 1886 eruption

The 1886 eruption was New Zealand's largest and most destructive historical volcanic event (Houghton and Wilson 1998). Basaltic magma was erupted from at least 50 discrete vents along a fissure that extended for 17 km and cut across the pre-existing Tarawera dome complex to the northeast and into the Rotomahana basin in the southwest, which hosted an active large geothermal system (Nairn 1979; Simmons et al. 1993; Fig. 2). About 0.8 km^3 of basaltic magma (DRE) was erupted in only five and a half h (Walker et al. 1984). This eruption deposited scoria up to 150 km, and ash up to 230 km downwind, to the northeast (Thomas 1888).

Chronology of the eruption

Eyewitness accounts of the 5.5-hour-long eruption were collected by (Smith 1886a,b) and (Williams 1887), and have been summarized by (Nairn 1979) and (Keam 1988). There had been few signs of unrest at Tarawera prior to 10 June 1886: Minor precursory activity included an increase in geothermal activity occurred at Lake Rotomahana and a 30 cm high wave on Lake Tarawera, early on the morning of 1 June 1886, which has been interpreted to have been caused by ground movement (Nairn 1979).

The most significant precursors were felt earthquakes which began 1 h prior to the onset of the eruption on 10

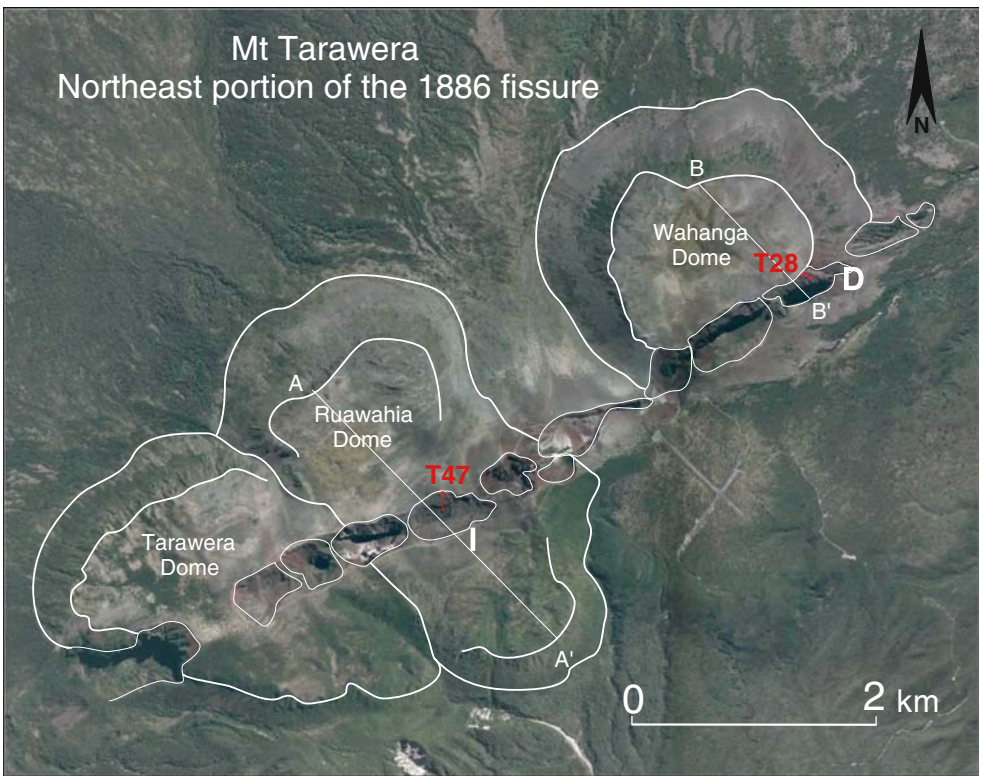

Fig. 3 Aerial photograph of Mt Tarawera and the northeastern portion of the 1886 fissure. *Thick white lines* define the margins of the Kaharoa domes and locations of key sections are shown *in red*. Craters are outlined *in thin white lines* and have been named A through L. Crater letters [*in white*] *mark craters* where sections described in this text are located. Cross section A-A′, B-B′ are shown in Fig. 4

June 1886. These earthquakes increased in intensity before the first outbreak (Nairn 1979), which began at 0130 (local time), in the vicinity of Wahanga, the northeastern-most of the Kaharoa domes (Fig. 2). Explosive activity then migrated southwestwards across Mt Tarawera. At 0210, a violent earthquake preceded the ascent of 'an enormous cloud of smoke and vapor ~9 km high' (Williams 1887). By 0230, the entire northeastern half of the fissure across Mt Tarawera (8 km in length) was in eruption, producing a >10 km-high plume. At 0330, eruptive activity spread to Rotomahana and a column of steam and ash higher than that at Tarawera ascended (Williams 1887). For the following 2.5 h, the entire 17 km length of the fissure (from Wahanga dome to Waimangu valley) was in eruption (Williams 1887). The eruption continued until 0600 on 10 June 1886. The most destructive phase of the eruption involved the generation of pyroclastic density currents of mud, ash and steam at Rotomahana which swept over 360 m-high hills and traveled radially 4–6 km from source (Nairn 1979).

This study

The focus of this paper is only the northeastern 8 km of the fissure which offers a unique opportunity to characterize and sample extremely proximal (>200 m) deposits of a short-lived, fissure-fed, basaltic Plinian eruption. These deposits form a series of half-cones along both sides of the northeastern half of the 1886 fissure, and emanated from numerous vents in at least 13 major craters across the top of Mt Tarawera (Fig. 3). Individual beds and groups of beds define complex wedging and off-lapping relationships, implying sudden shifts in eruptive intensity at adjacent vents (Sable et al. 2006). Here we examine the grain size and componentry of deposits from first the three contrasting phases of the eruption and second, the contrasting 'packages' of different dispersal within phase II, the climactic phase of activity.

Setting of the northeastern vents

The northeastern portion of the Tarawera fissure is formed by an en echelon array of 13 craters, which are separated by narrow (<20 m) septa (Nairn and Cole 1981; Sable et al. 2006). Walls of the craters are mostly sub-vertical with excellent exposures through the 1886 deposits into the underlying Kaharoa domes and pyroclastic units. The fissure walls within different craters have shown marked contrasts in stability within different craters, which persist to the present day. Some segments including craters D and

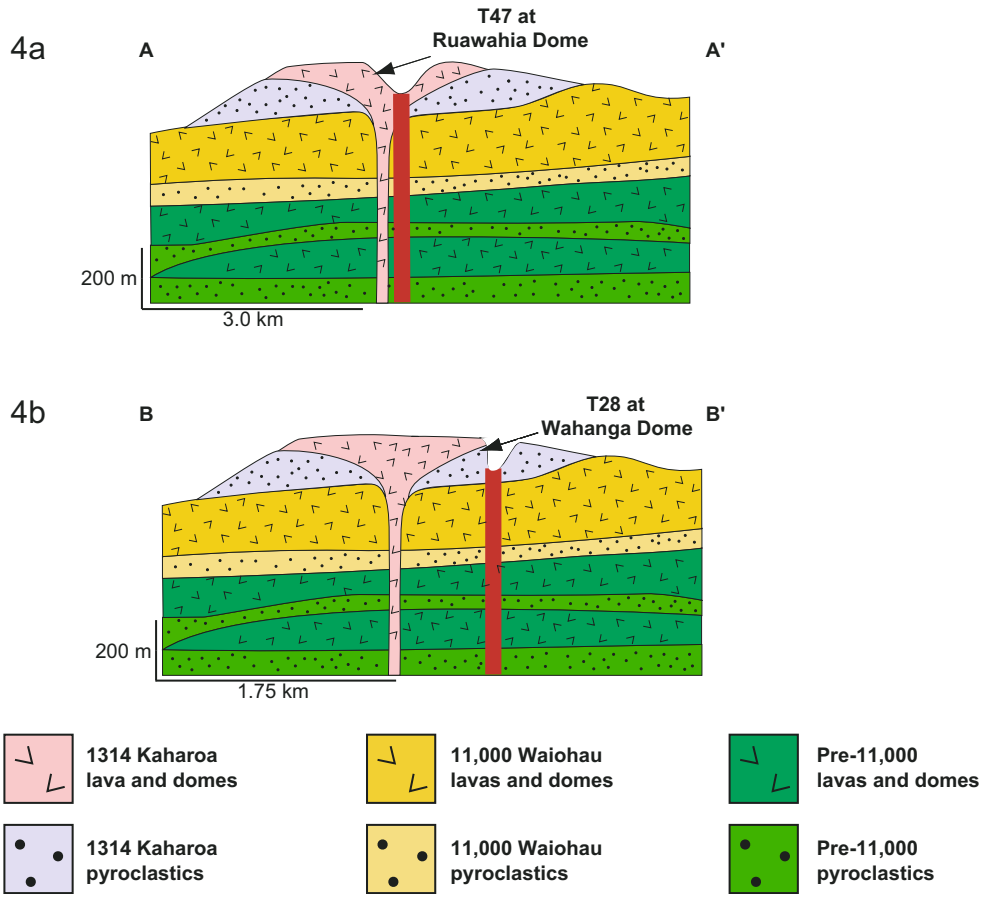

Fig. 4 Cross sections at two locations at right angles to the 1886 fissure through the basement stratigraphy of the 1314 A.D. Kaharoa, 11,000 ^{14}C yr B.P., and pre-11,000 yr lavas, domes and pyroclastics. Cross section A-A′ and B-B′ shows the position of the fissure in relation to the 1314 A.D. Ruawahia and Wahanga domes and related pyroclastics respectively (see Fig. 3). A-A′ is through crater I, adjacent to section T47, B-B′ is through crater D, adjacent to section T28. Note the different position of the fissure between the two sections relative to the 1314 A.D. Kaharoa domes. There is a greater abundance of Kaharoa pyroclastics versus lavas at section T28 and a steep inclination of the crater walls

E, remain highly unstable and subject to frequent rock falls, whereas near-vertical stable walls have remained since the close of the 1886 eruption in craters I, K, and L. Wall stability is related to the abundance of lava versus pyroclastic units in the Kaharoa 1314 AD deposits, which in turn reflects the relative location of the 1886 and Kaharoa vents. For example, the 1886 fissure cuts through the massive centers of both the Tarawera and Ruawahia domes (Figs. 2, 3, 4a) exposing thick, resistant, poorly jointed lavas and slices through the margin of Wahanga Dome exposing steep, well-jointed lava, dome breccias and pyroclastics (Fig. 4b).

1886 deposits

Previous work

All juvenile pyroclasts from the 1886 eruption were basaltic and the northeastern vents produced two geographically distinct tephra fall products (Houghton and Wilson 1998): (a) a tephra fall bed covering at least 10,000 km^2, erupted from northeastern Mt Tarawera vents (Fig. 3), and (b) the proximal, coarse-grained, cone-forming scoria fall deposit, confined to within c. 400 m of the Mt Tarawera craters (Fig. 5).

Walker et al. (1984) mapped the widespread scoria fall, and established its source. Mapping of the proximal tephra-fall units along the northeastern fissure (Nairn and Cole 1981; Houghton and Wilson 1998) identified more than 50 point sources that were active throughout the duration of the eruption and were the source for both products (a) and (b), above. This paper is concerned only with the proximal northeastern deposits (i.e. product (b) above). Walker et al. (1984) divided these deposits into five units. Further work by Houghton and Wilson (1998) suggested that these five units may be simplified into three, emphasizing the contrasts in style between the phreatomagmatic early and late eruptive phases (I+III), with the dominantly magmatic, more intense climactic phase II of the eruption. Throughout this paper we use phase to refer to a period of eruption (e.g. phase I, phase II etc) and unit to refer to deposits (unit 1, unit 2/3 etc).

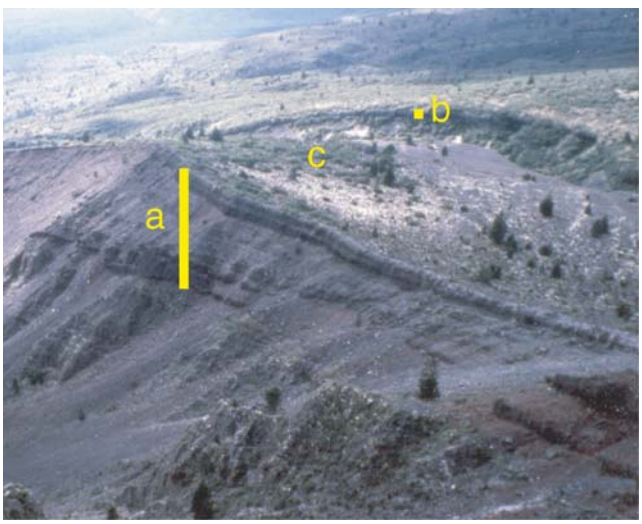

Fig. 5 Photograph showing rapid lateral thinning of the proximal deposits perpendicular to the 1886 fissure adjacent to crater D. The half cone geometry radially from the rift can be identified through thickness half distance measurements outboard from the rim, here outlined through measurements at sites (**a**) and (**b**). Measured thicknesses of the 1886 ejecta at (**a**) and (**b**) are 40 m and 2.8 m thick respectively. This rapid thinning imparts a steep primary dip to the proximal deposits (e.g. surface labeled (**c**)). Point sources of the explosion are to the left of figure within the 1886 fissure (not shown)

Sable et al. (2006) used deposit geometry to infer that vents along the fissure were erupting with contrasting intensities, with only four vents contributing significant material to the high Plinian plume. Sable et al. (2006) have proposed that the proximal deposits are mixtures of locally and regionally dispersed ejecta from at least three sources; (a) clasts which did not enter the Plinian plume but were sedimented from the gas thrust portion of the column; (b) particles that fell from close to the full height of the 1886 eruption plume; and (c) clasts erupted from adjacent vents which were in a lower intensity eruption style and not contributing significantly to the high plume.

Geometry, dispersal and stratigraphy

The northeastern proximal 1886 deposits consist of a series of truncated, partially overlapping scoria cones, or more accurately half-cones, which are confined to <400 meters from the centerline of the craters (Fig. 5). The deposits are well exposed and consist of a series of moderately to well-sorted lapilli-and-bomb beds with a total thickness between 35 and 75 m along the fissure. Most of the beds dip outwards away from the fissure and show rapid changes in thickness both parallel and perpendicular to the 1886 fissure (Sable et al. 2006; Figs. 5, 6).

The simplification of the stratigraphic units introduced by Walker et al. (1984), used in this paper is: phreatomagmatic unit 1; dominantly magmatic unit 2/3; phreatomagmatic unit 4/5. Each of these three units can be traced and correlated along the walls of the 8 km northeastern fissure segment. The units are further described and shown in Table 1 as follows:

(1) Unit 1, a black, phreatomagmatic scoria-fall deposit with moderately vesicular and sometimes quenched basaltic clasts, together with subordinate rhyolite wall-rock fragments erupted during phase I of the eruption.
(2) Unit 2/3, a bedded red and black scoria fall deposit with variable but generally low contents of rhyolitic wall-rock lithic clasts. The unit forms alternating welded

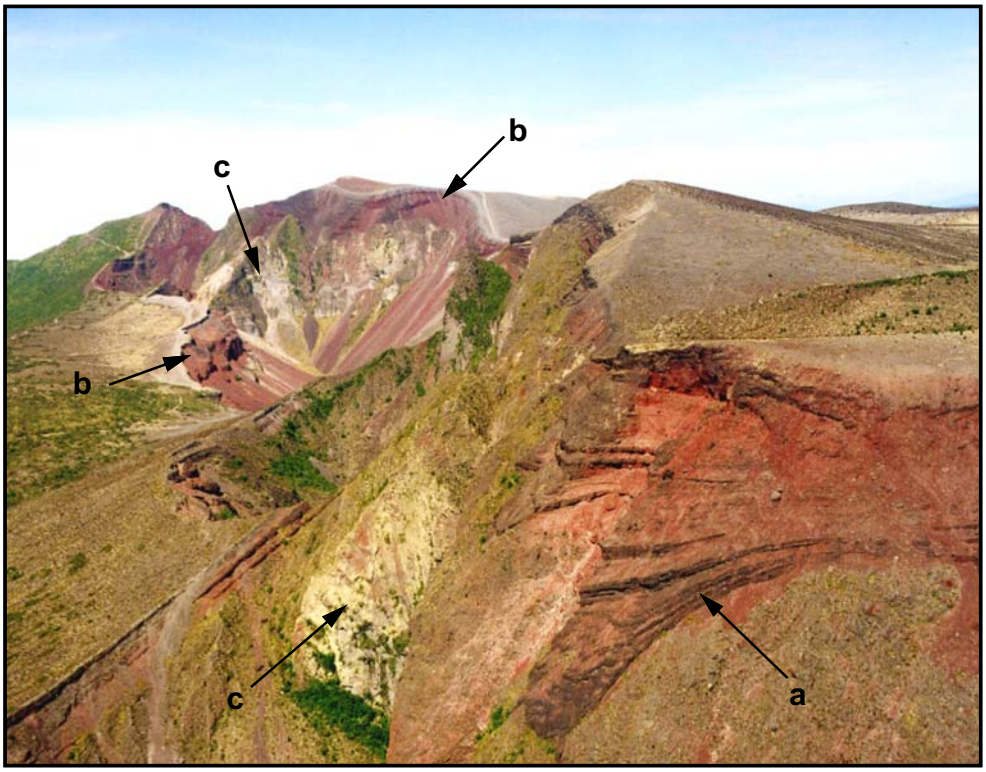

Fig. 6 Picture taken looking southwest along the 1886 fissure, adjacent to section T28 (see Fig. 3). Notice **a** the lenzoid, rapidly thinning nature of many beds and **b** the white color of unit 4/5 due to an abundance of rhyolitic Kaharoa lithic components. Pre-1886 rhyolitic lava of Wahanga dome and pyroclastic deposits of the Kaharoa eruption are exposed at (**c**)

and non-welded subunits that thicken and thin along the rift. We interpret this unit as the proximal equivalent, in time (phase II), of the widespread fall deposit.

(3) Unit 4/5, a white, phreatomagmatic lapilli-and-block rich unit dominated by rhyolite lithic fragments with subordinate dense quenched basaltic clasts, and sparse amounts of "Rotomahana Mud" (Nairn 1979), formed at the close of the eruption (phase III).

Lateral variations in the main Plinian phase

Houghton and Wilson (1998) presented field evidence that the widespread Plinian fall deposits largely accumulated during phase II, simultaneously with the proximal unit 2/3, rather than representing only the later stages of unit 2/3 accumulation (cf. Walker et al. 1984). However, along the fissure, the sequence of beds making up unit 2/3 varies greatly at different locations, in ways that are not immediately compatible with deposition from a classical Plinian plume (Sable et al. 2006). These lateral changes are primarily expressed in: (1) dispersal characteristics, with high variations of thinning rates of beds in crater walls parallel to the fissure; (2) variations in juvenile clast properties, i.e. grain size, vesicularity/density and morphology; and (3) content of wall-rock lithic clasts. A complication in interpreting proximal transport and deposition of pyroclasts is that all beds must also contain a mixture of clasts erupted from different point sources along the ca. 8 km long segment of the fissure (Sable et al. 2006).

Sable et al. (2006) have grouped beds of like character within proximal unit 2/3 into "packages," each consisting of several beds of similar dispersal. They recognized that at any one site, as well as between sites, packages can vary considerably in terms of dispersal, as reflected in thinning half distances. Some packages are characterized by smaller scale fluctuations in grain size and especially lithic clast content defining bedding on a meter scale (e.g. Fig. 7a), whereas other packages are relatively uniform throughout. Many beds contain a juvenile population of highly vesicular, ragged and fluidal scoria. Thinning half distances for these packages (typically 2–35 m) reflect the most rapid lateral changes in thickness. Other packages at the same site contain a wider range of juvenile clasts from ragged scoria to denser clasts with quenched surfaces. These packages commonly have longer thinning half

Table 1 Revision of units made by previous workers and their role in the current Tarawera nomenclature used in this study

Timing	Walker et al. 1984	Houghton and Wilson 1998	This study
phase I	unit 1	Early phreatomagmatic	unit 1
phase II	unit 2	Largely magmatic	unit 2/3
	unit 3		
phase III	unit 4	Late phreatomagmatic	unit 4/5
	unit 5		

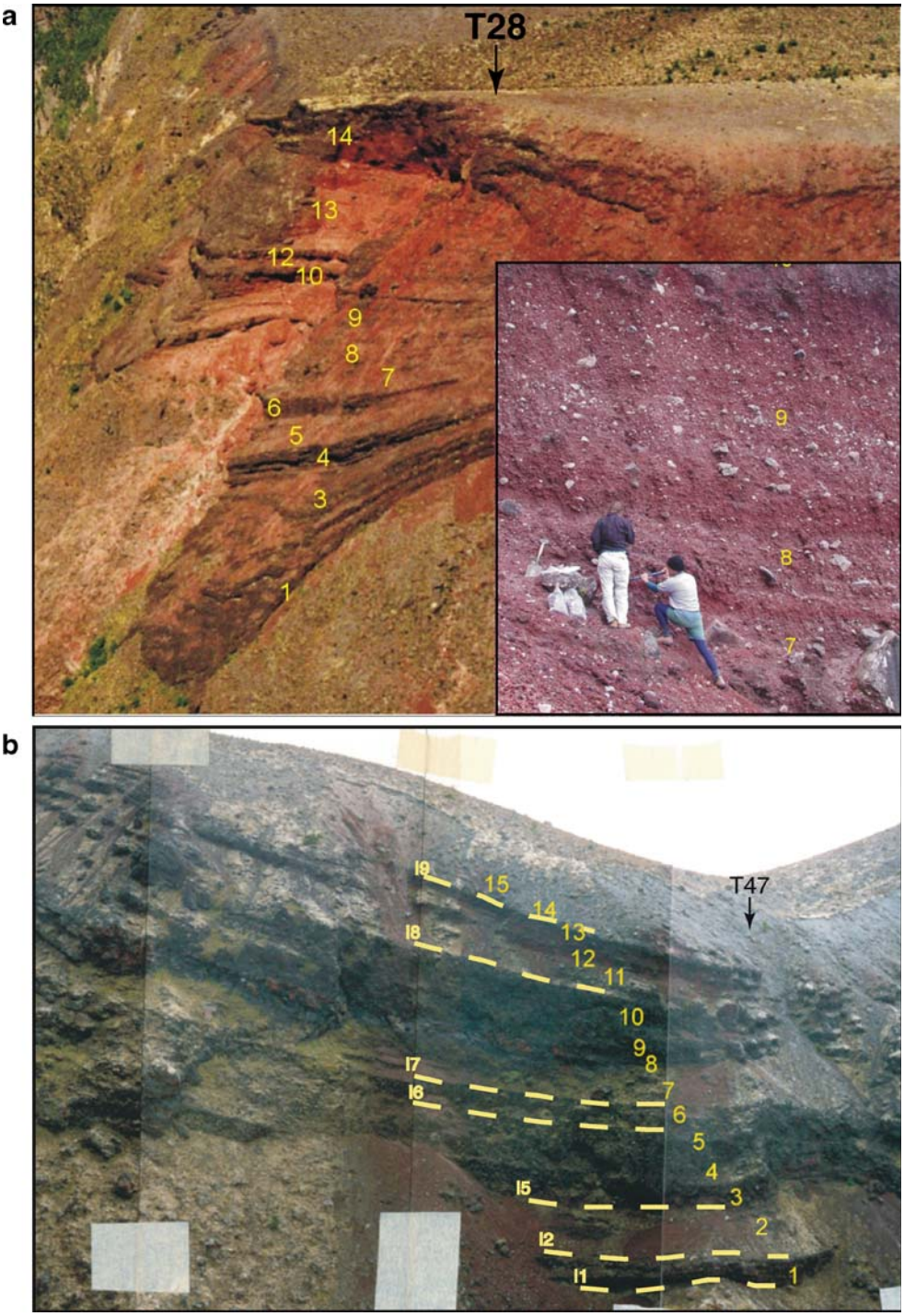

Fig. 7 **a** Photograph showing the five packages and 14 subpackages within unit 2/3 identified at section T28. Packages defined by Sable et al. (2006) are indicated by the crater letter (D) and number. Note the contrasting dispersal of adjacent packages. The location of the stratigraphic section T28 is identified by the *arrow*, in the reentrant in the middle of the photograph. Unit 1 is concealed in this image. Unit 4/5 is present as the *upper grey/white* unit overlying the red unit 2/3 deposits. The inset photo is representative of the non-uniformity of packages in terms of grain size and particularly lithic abundance within T28. *Yellow numbers* denotes subpackage number (see Fig. 8a). **b** Packages I1 through I9 and subpackages 1 through 15 within the Unit 2/3 deposits at section T47. Packages, as defined by Sable et al. (2006), are indicated by the crater letter (I) and number. Packages at this section can be traced along the fissure into adjacent craters. Note the sharp boundaries between welded and non-welded packages, resulting in cliff forming benches. The location of the stratigraphic section T47 is identified by the arrow

distances of up to 270 m. This study examines in more detail the nature of these complex proximal deposits based on two stratigraphic sections with packages that exhibit end-member examples of thinning half distances.

The studied sections

In Fig. 3, the locations of the two sections, 4 km apart, are shown: T28 from the east side of Wahanga dome and T47 from the southwestern side of Ruawahia dome. Section T28 comprises predominantly of rapidly thinning packages and is representative of the lower intensity end member (Sable et al. 2006; Figs. 7a, 8a). The more widely dispersed packages reflect a higher intensity of eruption, and contain an admixture of clasts from the margins of lower plume and jet with particles sedimented from the high plume (Sable et al. 2006), epitomized by T47 (Figs. 7b, 8b). The accumulation rates at the two endmember sections have been calculated

based on the thickness of each section and the total eruption duration of 5.5 h. The T28 accumulation rate is 5.1 m/h, versus an accumulation rate of 9.5 m/h at T47. These are likely underestimates since phase II probably only lasted for 4–4.5 h based on the chronology outlined above. We will discuss the implications for these very high values in a later section.

Section T28

This section exposes a vertical 28.1 m-thick sequence containing unit 1 and unit 2/3 deposits (Figs. 7a, 8a) in crater D (Fig. 3). Unit 4/5 is not present at this section due to erosion, however it was sampled <200 m to the southwest at T28a. In unit 2/3 we see a succession of well-bedded, non-welded to moderately welded, cone-forming beds, with rapid lateral thinning parallel to the fissure. Juvenile clasts are predominantly ragged with minor population of fluidal clasts. At T28, we observe an alternation of well bedded and uniform packages (Fig. 7a). Five packages of beds have been identified in unit 2/3 on this basis (Fig. 8a). These packages correspond to the least widely dispersed packages outlined in Sable et al. (2006) with a range of thinning half-distances from 20 to 35 m.

Section T47

This section has a vertical thickness of 52 meters in crater I (Fig. 3) and all three units are represented (Figs. 7b, 8b). Unit 2/3 deposits at this section are relatively homogeneous in comparison with T28: (1) packages do not thin as rapidly parallel to the fissure, (2) lithic content is generally poor and (3) beds have similar grain size characteristics. Juvenile clasts are predominantly ragged, although a minor proportion of clasts show 'knobbly' morphologies (Fig. 9). Seven relatively uniform packages have been defined for unit 2/3 deposits at T47 with thinning half distances of up to 270 meters (Sable et al. 2006; Fig. 8b).

Eruption sequences

Unit 1 The opening phase of the eruption produced phreatomagmatic fall deposits which vary from 0 to 4.3 m in thickness along the fissure. At T28, unit 1 rests on an irregular surface with at least 2 m of local relief in the surface rubble of Wahanga dome. It is 1.1 m thick and subdivided into four beds (Fig. 8a), with slight changes in grain size, lithic content, and morphologies of the juvenile clasts (vertical changes in juvenile clast morphologies are a significant feature of unit 1). At T47, unit 1 is 4.3 m thick and contains a great diversity of juvenile clast vesicularities and morphologies. Five beds are distinguished principally on the basis of minor changes in grain size characteristics (Fig. 8b).

Fig. 8 **a** Composite stratigraphic section and description for T28 and T28a proximal deposits. *Open symbols* are basaltic juvenile clasts and black symbols are rhyolite lithic clasts. Section heights are 28.1 meters (T28) and 2.9 meters (T28a). *Red arrows* indicate grain size sample locations. Numbers 1 through 14 are the sub-packages defined in this study. Packages defined by Sable et al. (2006) are indicated by crater letter (D) and number. The corresponding thinning half distance for each package is given below the package label in parenthesis. **b** Composite stratigraphic section and description for T47 proximal deposits. *Open symbols* are basaltic juvenile clasts and *black symbols* are lithic clasts. Section height is 52 meters. *Red arrows* indicate grain size sample locations. Numbers 1 through 15 are the sub-packages defined in this study. Packages and corresponding thinning half distance defined by Sable et al. (2006) are indicated by crater letter (I) and number in parentheses

Unit 2/3 At T28 unit 2/3 comprises five packages totaling 27 m of vertical thickness; each package is defined by sharp changes in bedding, componentry and juvenile clast vesicularity (Figs. 8a, 10a). Most packages are confined to only a small part of crater D, which is less than 500 m long. T47: Unit 2/3 at section T47 comprises of a 43.2 m thick sequence, which is divided into nine packages (Figs. 8b, 10b).The dispersal of every unit 2/3 package at T47 is greater than that of any package measured at T28. The vertical sequence of unit 2/3 deposits at T47 is relatively homogeneous with respect to dispersal, lithic content, grain size and sorting (Fig. 10b) and contrasts markedly in these respects with section T28.

Unit 4/5 At T28a, unit 4/5 deposits form a 2.3 m sequence of four ash-rich, poorly sorted beds (Fig. 8a). At T47, unit 4/5 is a 4.5 m thick very poorly sorted, coarse, matrix-poor bomb-and-block fall deposit (Fig. 8b).

Granulometry and componentry

Granulometric studies

In order to quantify lateral and vertical (i.e., temporal) changes in grain size, sections were sampled at each location, at irregular vertical intervals reflecting the stratigraphy. At least one representative sample was taken from each major bed. Samples were collected over very narrow vertical thickness intervals, typically two clast diameters and never more than three clast diameters. Sampling was initiated around the largest visible clast, which was extracted first. The weight of this coarsest clast was measured, and used to determine an appropriate size for a representative sample. All units were sieved and weighed in the field down to −4 φ (16 mm),and a representative split of the <16 mm fraction then taken to the laboratory for further analysis.

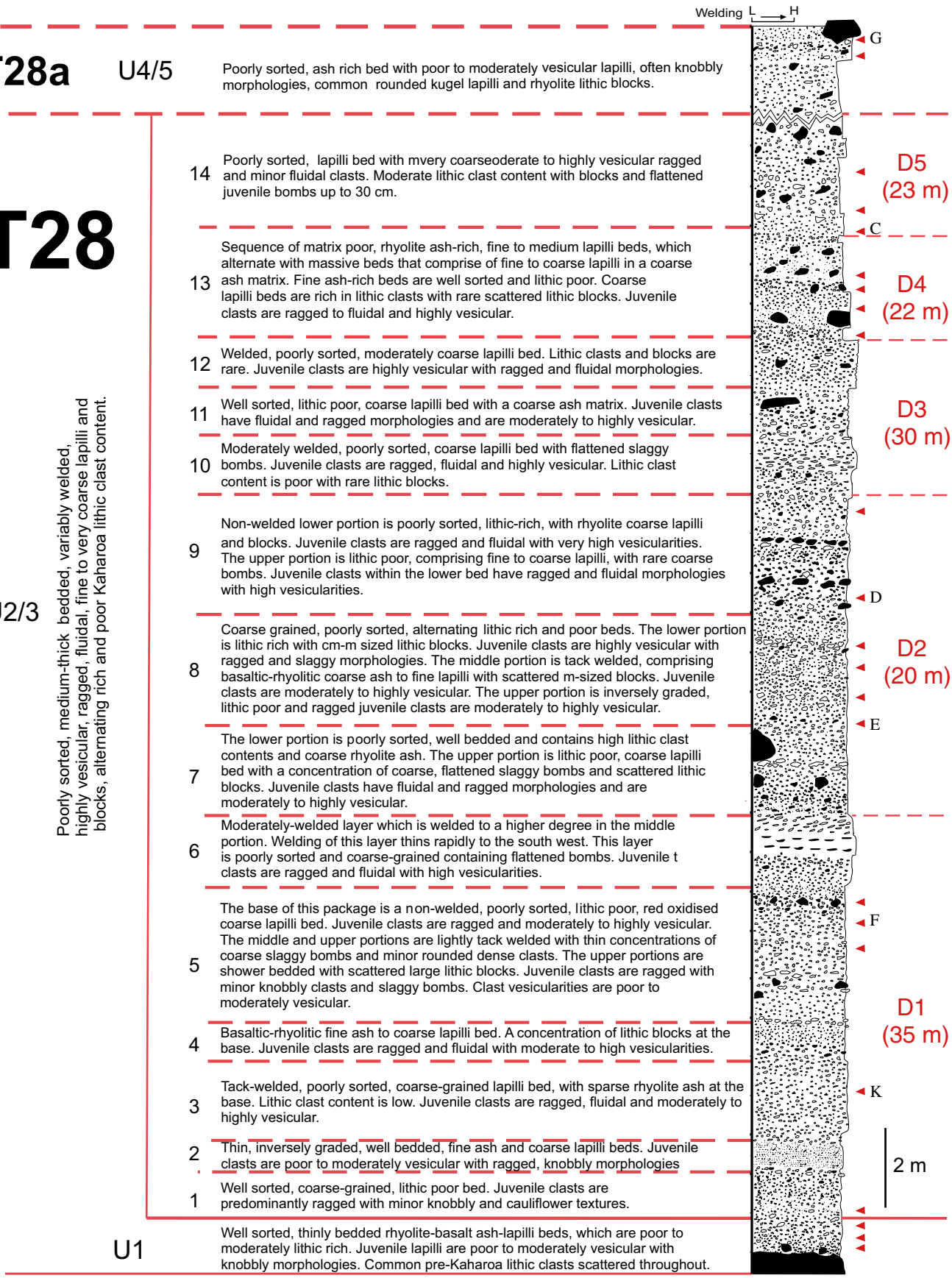
Welding L → H
T28a
U4/5
Poorly sorted, ash rich bed with poor to moderately vesicular lapilli, often knobbly morphologies, common rounded kugel lapilli and rhyolite lithic blocks.
T28
14 Poorly sorted, lapilli bed with mvery coarseoderate to highly vesicular ragged and minor fluidal clasts. Moderate lithic clast content with blocks and flattened juvenile bombs up to 30 cm.
13 Sequence of matrix poor, rhyolite ash-rich, fine to medium lapilli beds, which alternate with massive beds that comprise of fine to coarse lapilli in a coarse ash matrix. Fine ash-rich beds are well sorted and lithic poor. Coarse lapilli beds are rich in lithic clasts with rare scattered lithic blocks. Juvenile clasts are ragged to fluidal and highly vesicular.
12 Welded, poorly sorted, moderately coarse lapilli bed. Lithic clasts and blocks are rare. Juvenile clasts are highly vesicular with ragged and fluidal morphologies.
11 Well sorted, lithic poor, coarse lapilli bed with a coarse ash matrix. Juvenile clasts have fluidal and ragged morphologies and are moderately to highly vesicular.
10 Moderately welded, poorly sorted, coarse lapilli bed with flattened slaggy bombs. Juvenile clasts are ragged, fluidal and highly vesicular. Lithic clast content is poor with rare lithic blocks.
9 Non-welded lower portion is poorly sorted, lithic-rich, with rhyolite coarse lapilli and blocks. Juvenile clasts are ragged and fluidal with very high vesicularities. The upper portion is lithic poor, comprising fine to coarse lapilli, with rare coarse bombs. Juvenile clasts within the lower bed have ragged and fluidal morphologies with high vesicularities.
U2/3
Poorly sorted, medium-thick bedded, variably welded, highly vesicular, ragged, fluidal, fine to very coarse lapilli and blocks, alternating rich and poor Kaharoa lithic clast content.
8 Coarse grained, poorly sorted, alternating lithic rich and poor beds. The lower portion is lithic rich with cm-m sized lithic blocks. Juvenile clasts are highly vesicular with ragged and slaggy morphologies. The middle portion is tack welded, comprising basaltic-rhyolitic coarse ash to fine lapilli with scattered m-sized blocks. Juvenile clasts are moderately to highly vesicular. The upper portion is inversely graded, lithic poor and ragged juvenile clasts are moderately to highly vesicular.
7 The lower portion is poorly sorted, well bedded and contains high lithic clast contents and coarse rhyolite ash. The upper portion is lithic poor, coarse lapilli bed with a concentration of coarse, flattened slaggy bombs and scattered lithic blocks. Juvenile clasts have fluidal and ragged morphologies and are moderately to highly vesicular.
6 Moderately-welded layer which is welded to a higher degree in the middle portion. Welding of this layer thins rapidly to the south west. This layer is poorly sorted and coarse-grained containing flattened bombs. Juvenile t clasts are ragged and fluidal with high vesicularities.
5 The base of this package is a non-welded, poorly sorted, lithic poor, red oxidised coarse lapilli bed. Juvenile clasts are ragged and moderately to highly vesicular. The middle and upper portions are lightly tack welded with thin concentrations of coarse slaggy bombs and minor rounded dense clasts. The upper portions are shower bedded with scattered large lithic blocks. Juvenile clasts are ragged with minor knobbly clasts and slaggy bombs. Clast vesicularities are poor to moderately vesicular.
4 Basaltic-rhyolitic fine ash to coarse lapilli bed. A concentration of lithic blocks at the base. Juvenile clasts are ragged and fluidal with moderate to high vesicularities.
3 Tack-welded, poorly sorted, coarse-grained lapilli bed, with sparse rhyolite ash at the base. Lithic clast content is low. Juvenile clasts are ragged, fluidal and moderately to highly vesicular.
2 Thin, inversely graded, well bedded, fine ash and coarse lapilli beds. Juvenile clasts are poor to moderately vesicular with ragged, knobbly morphologies
1 Well sorted, coarse-grained, lithic poor bed. Juvenile clasts are predominantly ragged with minor knobbly and cauliflower textures.
U1
Well sorted, thinly bedded rhyolite-basalt ash-lapilli beds, which are poor to moderately lithic rich. Juvenile lapilli are poor to moderately vesicular with knobbly morphologies. Common pre-Kaharoa lithic clasts scattered throughout.
G
D5 (23 m)
C
D4 (22 m)
D3 (30 m)
D
D2 (20 m)
E
F
D1 (35 m)
K
2 m

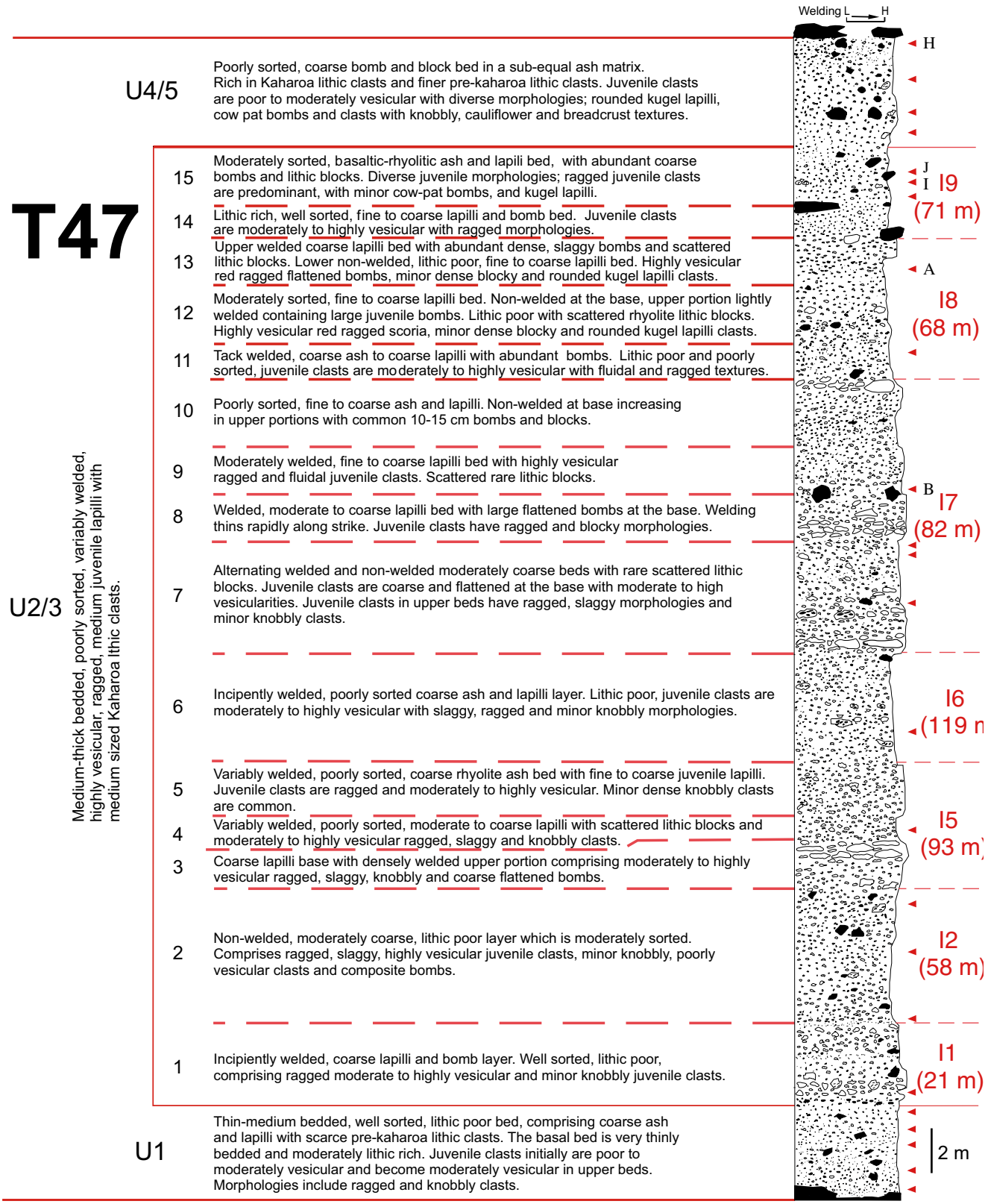

Fig. 8 (continued)

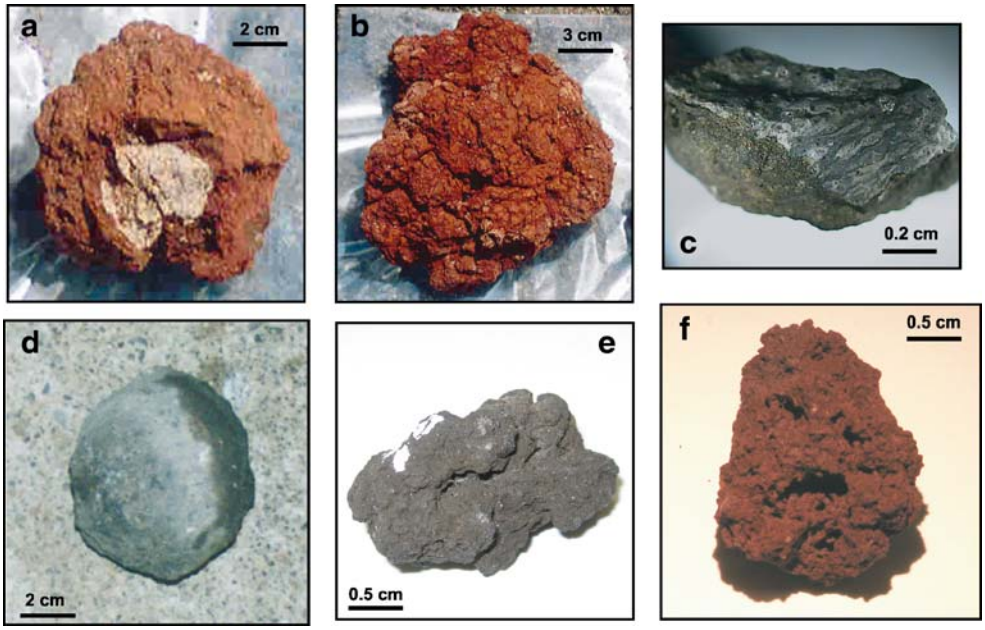

Fig. 9 Photos of clast morphologies described in the paper. (**a**) cored juvenile clast with Kaharoa lithic clast within. (**b**) cauliflower texture on a basaltic bomb, common in unit 4/5 deposits. (**c**) basalt-coated pre-Kaharoa clast, note the flow banding in the clast. (**d**) a cored spherical or 'kügel' basaltic bomb, common in unit 4/5 deposits. (**e**) a 'knobbly' clast, found commonly in unit 4/5 deposits. (**f**) a ragged juvenile clast, typical of unit 2/3 deposits

Unit 1 samples at both sections are distinguished by relatively good sorting (Inman sorting values σ_φ between 1.2 and 2.1 over a range of median grain size: Fig. 11a). Most samples from this unit are considerably finer $\left(\mathrm{Md}_\varphi = -1.1 \text{ to } -2.2_\phi\right)$ than that of overlying unit 2/3 (Fig. 11a, b). The median grain size of unit 1 at T47 is coarser than at T28 and only slighter finer than the overlying unit 2/3 beds (Fig. 10a, b). Unit 2/3 samples from T47 are more uniform in terms of grain size and somewhat better sorted than their T28 counterparts (Fig. 11b). At T28, the wide range in median diameters reflects an alternation of packages of alternating coarser and finer grain size $\left(\mathrm{Md}_\varphi = -1.8 \text{ to } -6.1_\phi\right)$ (Fig. 11b). There is no obvious change in sorting with change in median diameter. Samples from unit 2/3 at T47 are generally ash-poor (<2.7 wt% finer than 2 φ), moderately sorted $\left(\sigma_\varphi = 1.6 \text{ to } 3.2_\phi\right)$, lapilli beds $\left(\mathrm{Md}_\varphi = -2.4 \text{ to } -4.7\right)$ (Fig. 11b). Samples from unit 4/5 are markedly less well sorted than those of unit 1 $\left(\sigma_\varphi = 2.0 \text{ to } 3.8\right)$ (Fig. 11a), overlapping with those of T28 unit 2/3 deposits. The samples have a similar range of median diameters to unit 1 and unit 2/3.

Componentry

The main components were identified, separated and weighed within each phi interval., In the field, this was completed from −8 φ (256 mm) through −4 φ (16 mm) and in the laboratory to −2 ϕ (4 mm). Clasts were separated into: (1) juvenile basalt; (2) Kaharoa rhyolite lithics; (3) pre-Kaharoa rhyolite lithics; (4) basalt-coated Kaharoa rhyolite; and (5) basalt-coated pre-Kaharoa rhyolite.

Juvenile basalt clasts

Juvenile basalt clasts in the 1886 eruption deposits show greatly varying morphologies and vesicularities (Fig. 9). They are broadly categorized into two classes; (a) *Ragged scoria* are moderate to highly vesicular red, brown or black clasts with jagged rather than smooth fluidal shapes. (b) *Dense basalt lapilli/bombs* include: (1) breadcrusted clasts with glassy, brittle exteriors showing multiple cracks and fractures and moderately vesicular interiors, (2) gnarled, "knobbly" particles, with irregular cauliflower surface textures, sometimes chilled rinds and dense interiors, and (3) spherical, juvenile 'kügel' lapilli, which vary in size (4–64 mm), are dense and often have lithic cores. Commonly the spherical lapilli clasts have a composite structure consisting of multiple layers defined by sharp textural changes. A striking feature of all large juvenile clasts is that they contain varying amounts of visible rhyolitic fragments, typically mm to cm across.

Within the stratigraphic sequence, there are systematic variations in the nature of the juvenile clasts. In unit 1, basal juvenile clasts are black, spherical or knobbly. Moderately vesicular, ragged scoria become more abundant at the top of unit 1 (Fig. 8a, b). In unit 2/3, juvenile clasts have predominantly ragged or fluidal morphologies however, within the lower sequence, and particularly in widely dispersed packages, knobbly cauliflower clasts are also found. In unit 4/5, there is the greatest diversity of juvenile clast morphologies amongst the 1886 products, including dense bombs with cauliflower and breadcrust textures, kügel lapilli, dike-wall fragments and vesicular clasts with glassy and poorly vesicular rinds (Fig. 8a, b).

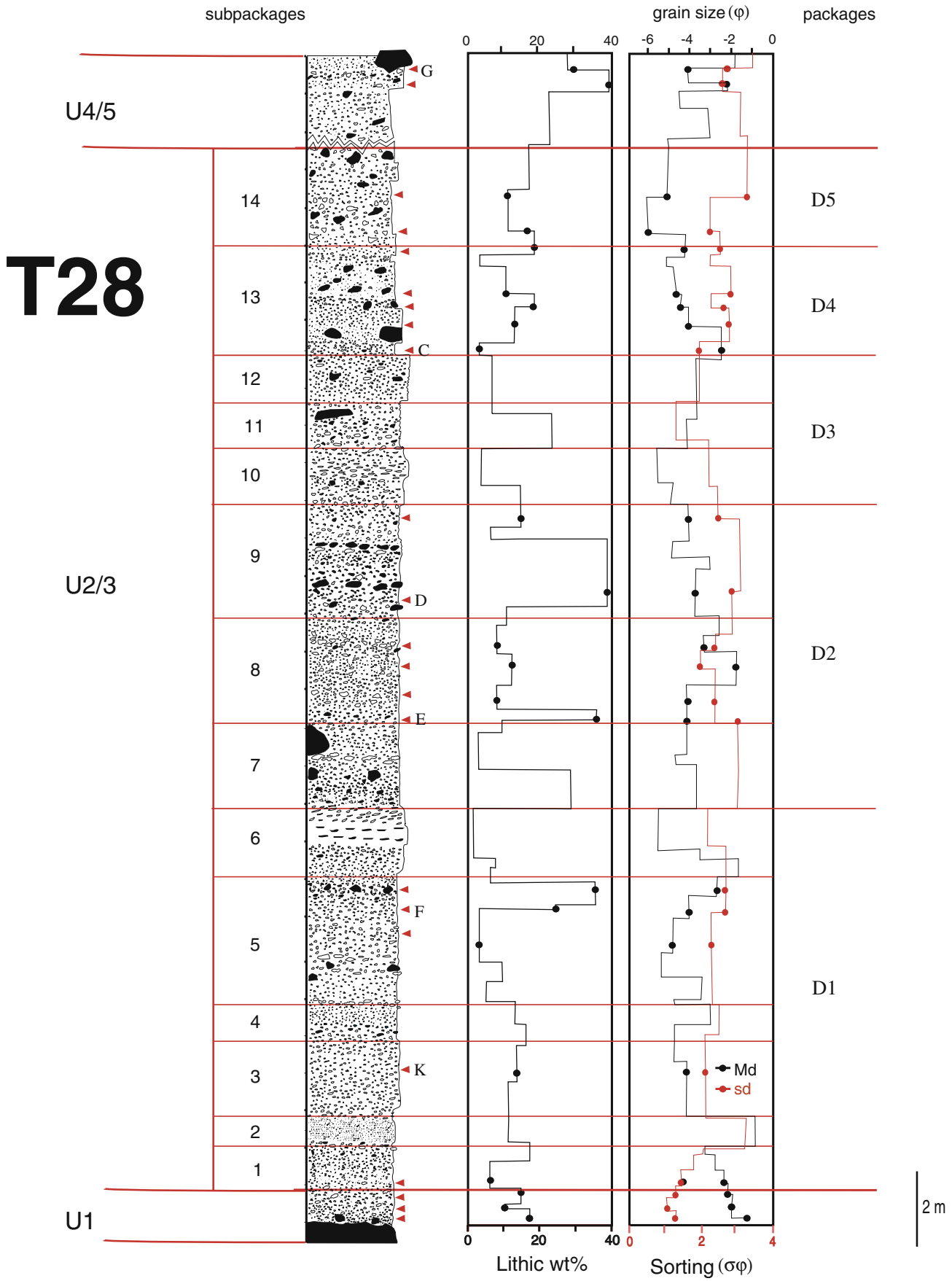
T28
subpackages
grain size (φ)
packages
U4/5
U2/3
U1
14
13
12
11
10
9
8
7
6
5
4
3
2
1
G
C
D
E
F
K
D5
D4
D3
D2
D1
Md
sd
0
20
40
-6
-4
-2
0
0
2
4
Lithic wt%
Sorting (σφ)
2 m

◀ **Fig. 10 a** T28 stratigraphy, lithic wt%, grain size and sorting characteristics of proximal deposits. Packages are after Sable et al. (2006) indicated by crater letter (D) and number. The *red triangles with letters* represent grain size samples that are referred to in the text. Note the coarsening of grain size with stratigraphic height throughout unit 1. T28 is also characterized by a high and fluctuating wall rock lithic content throughout unit 2/3. **b** T47 stratigraphy, lithic wt%, grain size and sorting characteristics of proximal deposits. Packages are after Sable et al. 2006 indicated by crater letter (I) and number. The *red triangles with letters* represent grain size samples that are referred to in the text. Note the decreasing abundance of wall rock lithic content with time through unit 1. T47 is consistently poor in wall rock lithic content throughout unit 2/3 relative to T28

Wall-rock lithics

The wall rock lithic fragments incorporated into the 1886 fall deposits consist of two distinct types: (a) *1314 AD Kaharoa rhyolite clasts* are glassy and phenocryst-rich (10–25%), containing plagioclase, quartz, conspicuous biotite and minor amphibole, orthopyroxene and Fe–Ti oxides (Leonard et al. 2002). These clasts may be pumiceous or dense, and are mostly fresh or occasionally hydrothermally altered. (b) *Pre-Kaharoa rhyolite clasts* are almost entirely lavas, derived from a combination of the 11,000, 15,000 and 18,000 ^{14}C yr B.P. eruption episodes that built much of the edifice of Mount Tarawera (Nairn 2002). These clasts can be distinguished from the Kaharoa rhyolite on the basis of their low phenocryst contents, devitrified nature, common flow banding and spherulitic textures. They are commonly hydrothermally altered but not readily distinguished from each other. Clasts of both Kaharoa and pre-Kaharoa lithologies are occasionally coated by single or multiple layers of dense basalt of varying thicknesses (Fig. 9). We present data for the samples in the form of trends with stratigraphic height (Figs. 10a, b, 12) and a plot of total lithic abundance versus relative combined abundance of Kaharoa and coated Kaharoa versus pre-Kaharoa and coated pre-Kaharoa rhyolite (Figs. 13a, b).

Results

Unit 1 Unit 1 is characterized by consistent moderate levels of wall rock abundance (6–18 wt%; Fig. 13a) and a range of relative abundance of Kaharoa (i.e., shallow <300 m) and pre-Kaharoa (deep: >300 m) material. Both parameters changed systematically with time, such that the total lithic abundance is highest in the basal beds (Figs. 10a, b) and these deposits also contain the highest abundance of pre-Kaharoa (i.e., deep-derived) clasts (Fig. 12). At T28, the first bed has the greatest abundance of pre-Kaharoa rhyolite (5.4 wt%), which gradually decreases (to 0.8 wt%), and persists as only a minor component (<1.8 wt%) within unit 2/3 (Fig. 12). At T47, the abundance of older pre-Kaharoa lithic clasts is higher also within the initial bed (7 wt%) than other beds in unit 1 (Fig. 12).

Unit 2/3 There are marked differences between the lithic populations in unit 2/3 at sections T28 and T47 (Fig. 13b). At T28, Kaharoa lithic clasts are dominant and pre-Kaharoa clasts always represent <2 wt% of the lithic population (Fig. 12). The total lithic abundance fluctuates rapidly over short vertical intervals, over a range from 3.5 to 45 wt% (Fig. 10a). At T47, the lithic content within unit 2/3 beds is much lower (<8 wt%), with the exception of the final package (Fig. 10b). At T47, the relative abundance of Kaharoa clasts varies widely, but is typically lower than for T28.

Unit 4/5 The relative abundance of Kaharoa-derived clasts is very high in all unit 4/5 samples, especially in comparison to unit 1, and total lithic content is high (Fig. 13a). In particular, at T47, wall-rock lithic contents in unit 4/5 increase systematically upwards, from 16.6 to 74.9 wt% (Fig. 10b). The abundance of pre-Kaharoa lithic clasts is initially < 0.25 wt% and then increases to 9.2 wt% in the uppermost sample (Fig. 12).

Juvenile clast vesicularity

A detailed vesiculation study of the 1886 basaltic scoria is presented in Sable et al. (in preparation). Bulk vesicularity data are summarized in Table 2 from that paper. A comparison of the vesicularity and vesicle size distribution of the clasts from the cone-forming and Plinian strongly suggest very similar ascent histories for the magma at T47 and T28 (Sable et al. (in preparation)).

Interpretation and discussion

Accumulation rates inferred for phase II

The dispersal characteristics of deposits at section T28, with thinning half distances of packages ranging from 22 to 35 m suggests that sedimentation at this site was dominated by vents that were in a weaker fountaining eruption style with limited incorporation of material produced and sedimented from either the lower portions of the Plinian column or the high plume. Thus the accumulation rate represents predominantly material produced from the adjacent low intensity vents with limited input from any Plinian vent. The T28 accumulation rate calculated over a total eruption duration of 5.5 h, is 5.1 m/h. In comparison, the widespread end member T47 with package thinning half distances between 29 and 119 m, has a time-average

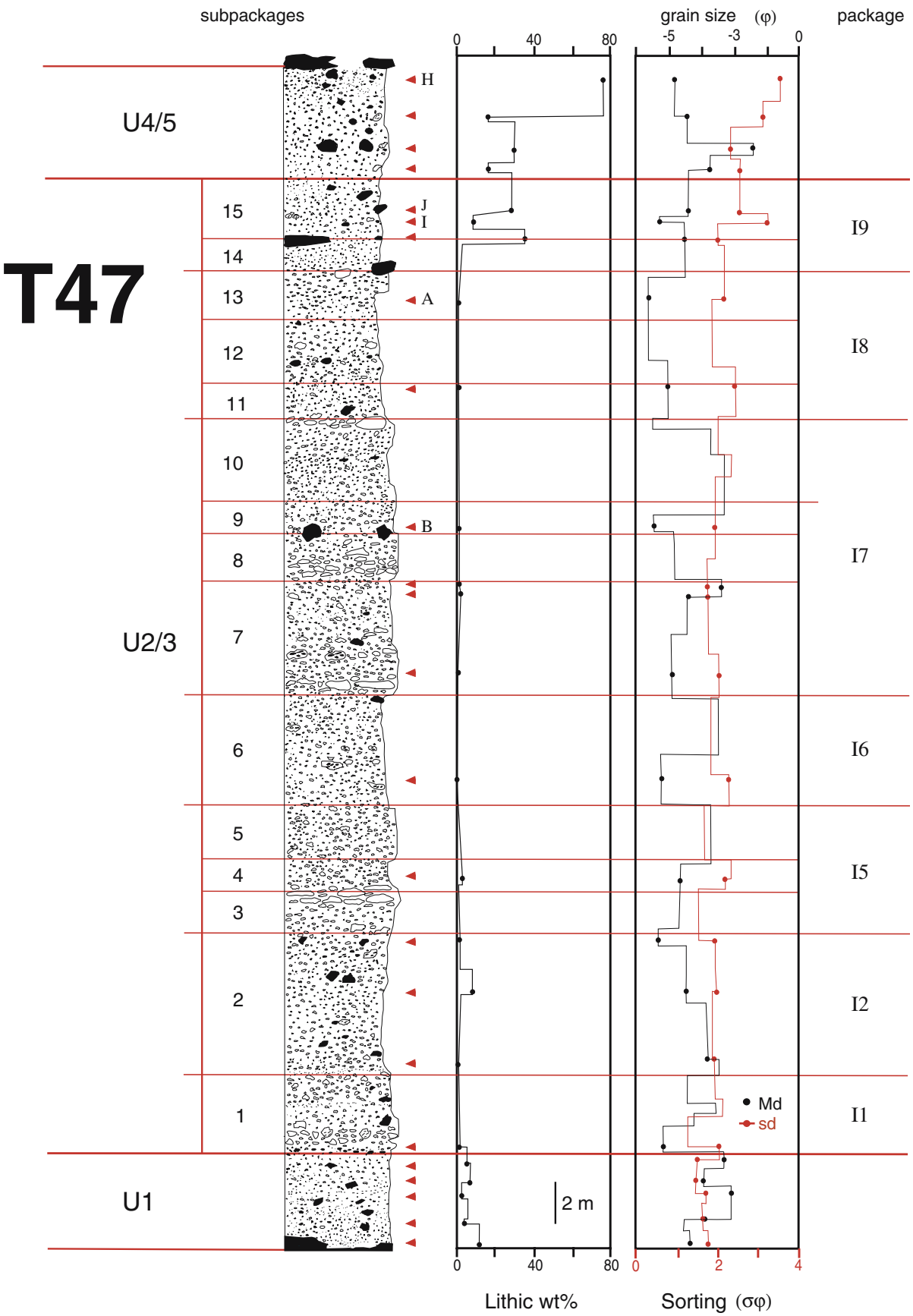
T47
subpackages
grain size (φ)
package
U4/5
U2/3
U1
H
J
I
A
B
15
14
13
12
11
10
9
8
7
6
5
4
3
2
1
I9
I8
I7
I6
I5
I2
I1
0
40
80
-5
-3
0
2 m
Md
sd
0
2
4
Lithic wt%
Sorting (σφ)

◀ **Fig. 10** (continued)

calculated accumulation rate of 9.5 m/h. The rate of accumulation for the cone-forming deposits like T28 is particularly interesting in the light of growth rates for Hawaiian and Strombolian cones. Houghton et al. (2006) calculate growth rates of 0.15–0.22 m/h for four recent historical eruptions of Etna and Kilauea. The 1886 cones thus accumulated at more than on order of magnitude higher rates implying mass fluxes much greater than those seen in simple cone-building eruptions.

Contrasts between phreatomagmatic phases (I and III) and climactic phase II

Grain size variations of tephra fall deposits are valuable in distinguishing the products of dry eruptions (e.g., Strombolian, Plinian) from those of phreatomagmatic eruptions, particularly those with high water/magma ratios (e.g., Surtseyan; Walker 1973). While deposits resulting from phreatomagmatic explosion involving high water/magma ratios are extremely fine grained and distinctly poorly sorted (Houghton and Nairn 1991), those resulting from low water/magma ratios are commonly coarse and relatively well sorted (Houghton and Hackett 1984; Houghton and Schmincke 1989; Houghton et al. 1999), and may plot in the strombolian and Plinian grain size fields of Walker and Croasdale (1972) and Walker (1973).

It is therefore not surprising that the grain size fields for all three 1886 units overlap partially on plots of median grain size versus sorting coefficients (Fig. 11a, b) with the implication that water/magma ratios were probably low to moderate for phases I and III. However samples collected from phreatomagmatic units 1 and 4/5 have

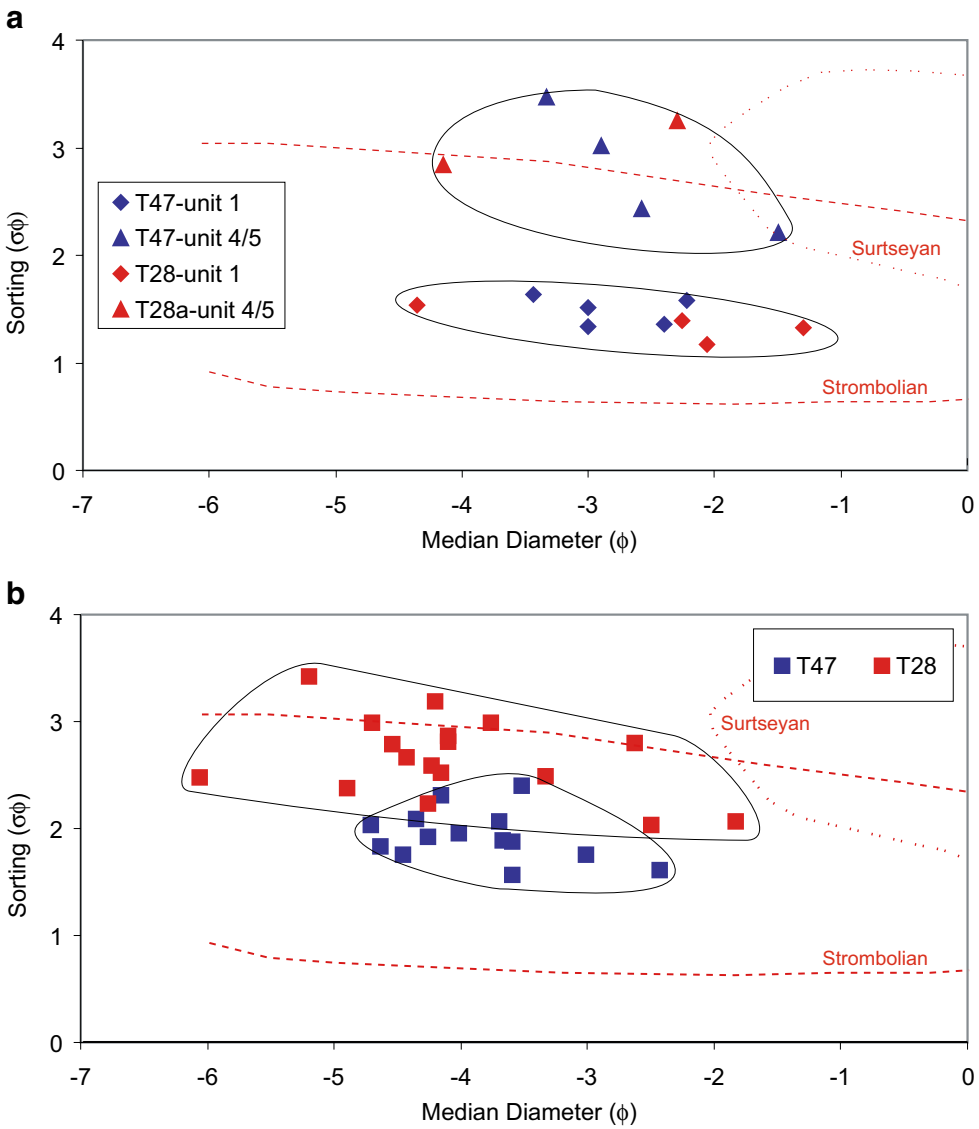

Fig. 11 **a** Median diameter (Md_{φ}) vs. sorting for unit 2/3 from sections T28 (*red*) and T47 (*blue*). Samples from unit 1 at both sites share common characteristics, as do unit 4/5 samples. Unit 4/5 samples are markedly more poorly sorted than those of unit 1. Fields of Walker and Croasdale (1972), modified by Cas and Wright (1987) for strombolian and surtseyan deposits have been outlined in red. **b** Median diameter vs. sorting for unit 2/3 from sections T28 (*red*) and T47 (*blue*). Note the marked contrast in sorting between the two sections and greater variability in sorting for section T28 than T47. Fields of Walker and Croasdale (1972), modified by Cas and Wright (1987) for strombolian and surtseyan deposits have been *outlined in red*

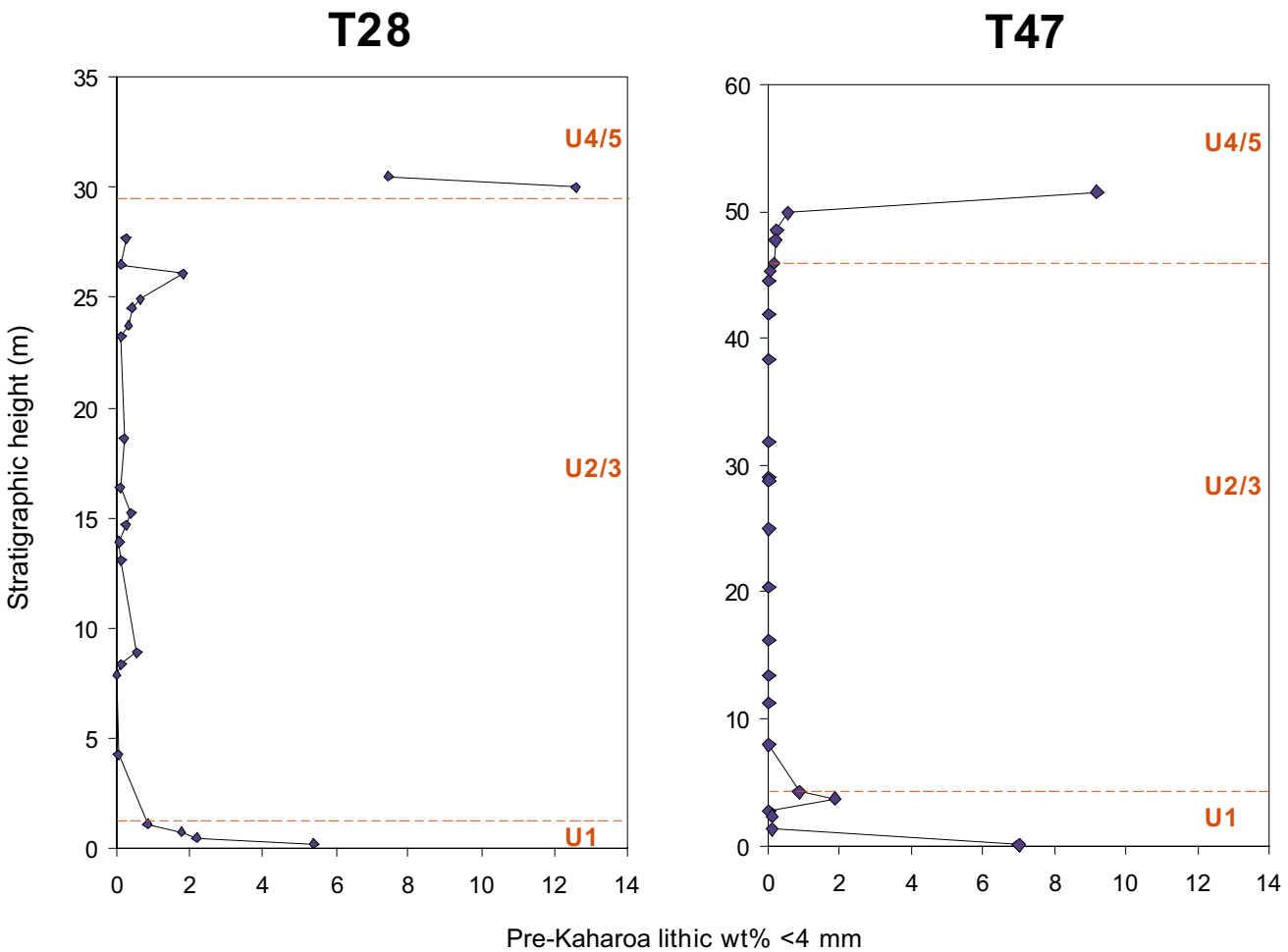

Fig. 12 Abundance of pre-Kaharoa lithic clasts (including basalt-coated pre-Kaharoa clasts) versus stratigraphic height for sections T28 and T47. Notice the trend of decreasing pre-Kaharoa lithic abundance with time in unit 1 deposits at both sections. Unit 4/5 samples have high (T28) or increasing (T47) pre-Kaharoa lithic clast contents. Unit 4/5 at T28 was sampled at a proximal adjacent location (T28a)

grain size characteristics that are distinctly different both from each other and from those of the main unit 2/3 of phase II. Unit 1 has similar grain size characteristics at T28 and T47 (Table 3) and is consistently better sorted (1.1–1.5 φ) than units 2/3 and 4/5. Unit 2/3 at both sections is both coarser-grained and more poorly sorted (Fig. 10a, b) than unit 1 but there are distinct differences between the sections. At T47 the grain size distributions of all samples are very similar with a peak at −4 to −6 φ and skewed towards fine particle size (Fig. 14a2, b2). The wall rock lithic content is low and shows a similar size distribution to the juveniles clasts (Fig. 14a1, b1). In contrast samples from T28 are of two types- (1) lithic-poor skewed unimodal samples (Fig. 14c1, c2) which are typically 1–2 phi units finer that the T47 samples and (2) lithic-rich samples which are often bimodal (Fig. 14d-f). The latter have modes at −6 to −7 φ and at −4 φ (Fig. 14d-f). The coarse mode is dominated by lithic blocks and removal of the >4 mm lithic subpopulation from the grain size samples produces size distributions very similar to the T47 samples (Fig. 14d1, e1, f1 versus d2, e2, f2).

Samples from unit 4/5 possesses a similar range of median grain size values to the T28 unit 2/3 deposits but are the least well sorted $\left(\sigma_{\varphi} = 2.2 \text{ to } 3.5\right)$ of the 1886 products. The poor sorting of unit 4/5 beds reflects a very wide range of particle sizes amongst the wall rock lithic population from coarse ash to blocks (Fig. 14g, h).

Changes with time within phases

Samples from unit 1 at T28 show a simple coarsening with stratigraphic height (Fig. 10a). There is then an abrupt ~2 φ shift to much coarser clasts at the unit 1-unit 2/3 contact, that is consistent with the idea that unit 2/3 was erupted primarily from vents which were erupting in a "dry" magmatic fashion (Sable et al. 2006). Within unit 2/3 there are abrupt changes in both median diameter and sorting between adjacent packages and even between beds (Fig. 10a, b) as discussed above. This pattern is consistent with rapid yet reversible changes in the nature of the clast population being ejected from these vents.

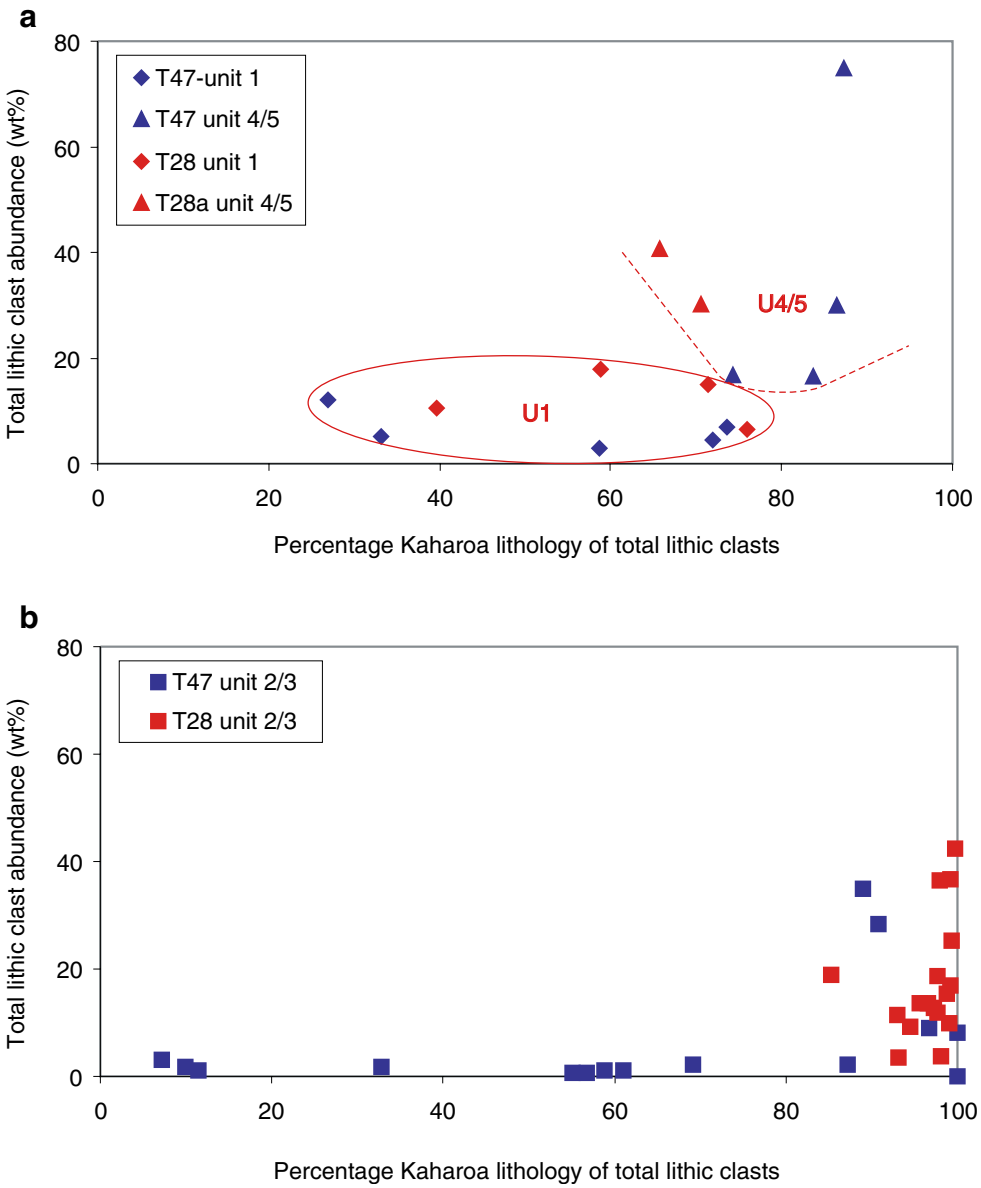

Fig. 13 **a** Percentage of Kaharoa lithic clasts (including coated Kaharoa clasts) vs. total lithic abundance for unit 1 and unit 4/5 deposits at sections T28 (*red*) and T47 (*blue*). Unit 1 beds from both sections have a similar distribution of the proportions of Kaharoa clasts. Deposits from unit 4/5 at both sections have higher total lithic clast abundance than unit 1 and a higher proportion of those are of Kaharoa lithology. **b** Percentage of Kaharoa lithic clasts (including coated Kaharoa clasts) vs. total lithic clast abundance for unit 2/3 deposits at sections T28 (*red*) and T47 (*blue*). Most T47 samples have low total lithic abundance and there is a wide range of abundance of Kaharoa clasts. T28 samples have a greater variability but typically higher total lithic abundance. Notice the dominance of Kaharoa clasts (>80%) within unit 2/3 deposits at section T28

At T47, the transition between units 1 and 2/3 shows an increase in median grain size from −2.4 to −4.3 phi (Fig. 10b), again consistent with the inferred abrupt shift in eruptive style from phreatomagmatic to magmatic (Walker et al. 1984). The consistent grain size and sorting of the following unit 2/3 beds suggest relatively uniform and steady-state eruptive conditions in comparison to site T28 (Fig. 10a, b). There is however a general trend of coarsening grain size with relatively uniform sorting values up to sample T28 K, (Fig. 10a) which fits with inferences of increasing eruptive vigor with time from eyewitness accounts (e.g., Williams 1887) and from other deposit characteristics (Sable et al. 2006). Unit 4/5 samples show a progressive shift towards coarser grain size and poorer sorting. Poor to very

Table 2 Summary of mean density values for stratigraphic units of the 1886 eruption taken from Sable et al. (in preparation)

	Unit 1	Unit 2/3	Unit 4/5
T28	1,400 (51%)	800–1,220 (58–72%)	1,900–2,080 (28–35%)
T47	1,140–2,000 (31–61%)	1,050–1,380 (52–64%)	1,590–1,790 (38–45%)

All density measurements have units of kg/m^3. Equivalent bulk vesicularities are shown (in brackets). Number of measured clasts; T28: unit 1=100, unit 2/3=1,600, unit 4/5=200; T47: unit 1=400, unit 2/3=1,500, unit 4/5=400.

Table 3 Summary grain size parameters for stratigraphic units of the 1886 eruption

Parameter	Unit 1	Unit 2/3	Unit 4/5
Mean diameter (Md_φ)	−1.1–−3.4	−1.8–−6.1	−1.4–−4.0
Sorting coefficient σ_φ	1.2–1.4	1.6–3.2	2.2–3.4
Skewness (φ)	−0.04–0.32	−0.02–0.26	0.05–0.34

poor sorting of the unit 4/5 deposits is due to the mixing of outsized lithic blocks with lapilli and ash particles. We interpret this grain size data as reflective of vent wall material falling into the vent during this period of decreasing magma supply.

Contrasts within the deposits of phase II

Within deposits of unit 2/3 at each section, groups of beds with (a) uniform or (b) non-uniform grain size and componentry characteristics and similar thinning half distances were grouped by Sable et al. (2006) into packages. Grain size analyses of samples taken throughout this unit reveal contrasts between packages with high and low thinning half distances at T47 and T28, respectively. T28 samples tend to be distinctly less well sorted than T47 samples, and sorting coefficients decrease slightly with decreasing grain size for T47 and more steeply for T28 samples (Fig. 11b). The samples from T47 are very low in wall rock lithics and show relatively simple unimodal grain size distributions, such as typically shown by sample B (Fig. 14). At T28, the poor sorting and coarse grain size throughout unit 2/3 partly reflects a coarse-grained lithic subpopulation (Fig. 14), that is two to four phi units coarser than the mean grain size of the juvenile clast subpopulation. Removal of this coarse lithic subpopulation from the clast assemblage generates a broad unimodal distribution only slightly less well sorted than the T47 samples (e.g. Fig. 14). This decreased sorting reflects a decoupling of a slightly coarser lithic and a finer juvenile population, which cannot be explained in terms of aerodynamic equivalence and density fractionation during transport. We suggest below that the decoupling of lithic and juvenile size is a function of the former being derived from collapse of the unstable portions of the vent walls adjacent to crater D. The grain size distribution of the juvenile clast population is consistent with the inference that explosions at this site were weaker than those recorded in the deposits at T47 (Sable et al. 2006).

Contrasts of wall rock content between phreatomagmatic phases I and III

The abundance and size of lithic clasts within unit 1 is strikingly similar between sections 28 and 47. Within unit 1, the basal bed at both sections has the highest abundance of both Kaharoa (Fig. 10a, b) and pre-Kaharoa lithic clasts (Fig. 12), which then decline in abundance through overlying unit 1 beds. Even more distinctive is the high relative abundance of pre-Kaharoa to Kaharoa lithic clasts (Fig. 12). The transition between unit 1 and unit 2/3 can be easily overlooked in terms of absolute lithic abundance, i.e., at T47 the consistent minor decrease of lithic abundance continues and at T28 there is no distinct change in absolute lithic abundance. However, the relative abundance of pre-Kaharoa clasts within unit 2/3 drops markedly (Fig. 12). In addition, data on lithic proportions and lithologies from units 1 and 4/5 show that the units occupy two different fields (Fig. 13a, b). The lithic populations within unit 1 have low total abundances, which are less dominated by Kaharoa clasts. Unit 4/5 samples have higher total lithic clast abundances and are proportionately richer in Kaharoa clasts (Fig. 13a, b).

These observations are consistent with early explosive fragmentation of the unit 1 magma beginning at depths greater than 300–400 meters, below the surficial Kaharoa country rock, incorporating relatively high amounts of pre-Kaharoa lithic clasts (Fig. 15). The decreasing trend of lithic clast abundance within unit 1 is the result of conduit excavation and stabilization. During the unit 4/5 stage, magma withdrawal facilitated a drop in the fragmentation surface, and accompanying explosions cleared and widened the vents facilitating the incorporation of large amounts of clasts derived from the Kaharoa domes (Fig. 15).

Contrasts of wall rock abundance in phase II

Between the two sections, there is a striking contrast in wall-rock lithic abundance in unit 2/3 (Fig. 10a, b). At T47, the lithic clast abundance is <8 wt% for the initial 14 sub-packages and only the last package is lithic-rich, marking a

Fig. 14 Total grain size histograms (juvenile plus lithic) (*left graphs*) and juvenile only histograms (*right graphs*) for six unit 2/3 samples and two unit 4/5 samples from both T28 and T47 to show the effect of outsized wall rock lithic clasts. Componentry for size fractions greater than 4 mm is superimposed on the histograms. *Blue and red colors* denote juvenile and lithic abundances respectively. In the right hand graphs for each sample, we have removed the coarse lithic fraction to better compare the grain size distributions of the juvenile clasts. *Letters to the right of graphs*, denote the sample locations (see Fig. 10a, b). The T47 unit 2/3 histograms have a coarser mode (−5 φ) than the T28 unit 2/3 samples (−2 to −4 φ) and are consistently low in wall rock abundance. Note how within the T28 unit 2/3 samples there are two different types of distributions: a unimodal distribution with no real change in the histogram when excluding lithic clasts (c) and distributions that are bimodal with a lithic mode at −7 φ and juvenile mode at −4 φ (d-f). The coarse mode of the lithic population in T28 unit 2/3 beds is due to a distinct population of wall rock lithic blocks. The phreatomagmatic unit 4/5 samples have a polymodal distribution and, similar to theT28 unit 2/3 samples, a distinct population of coarse lithic blocks

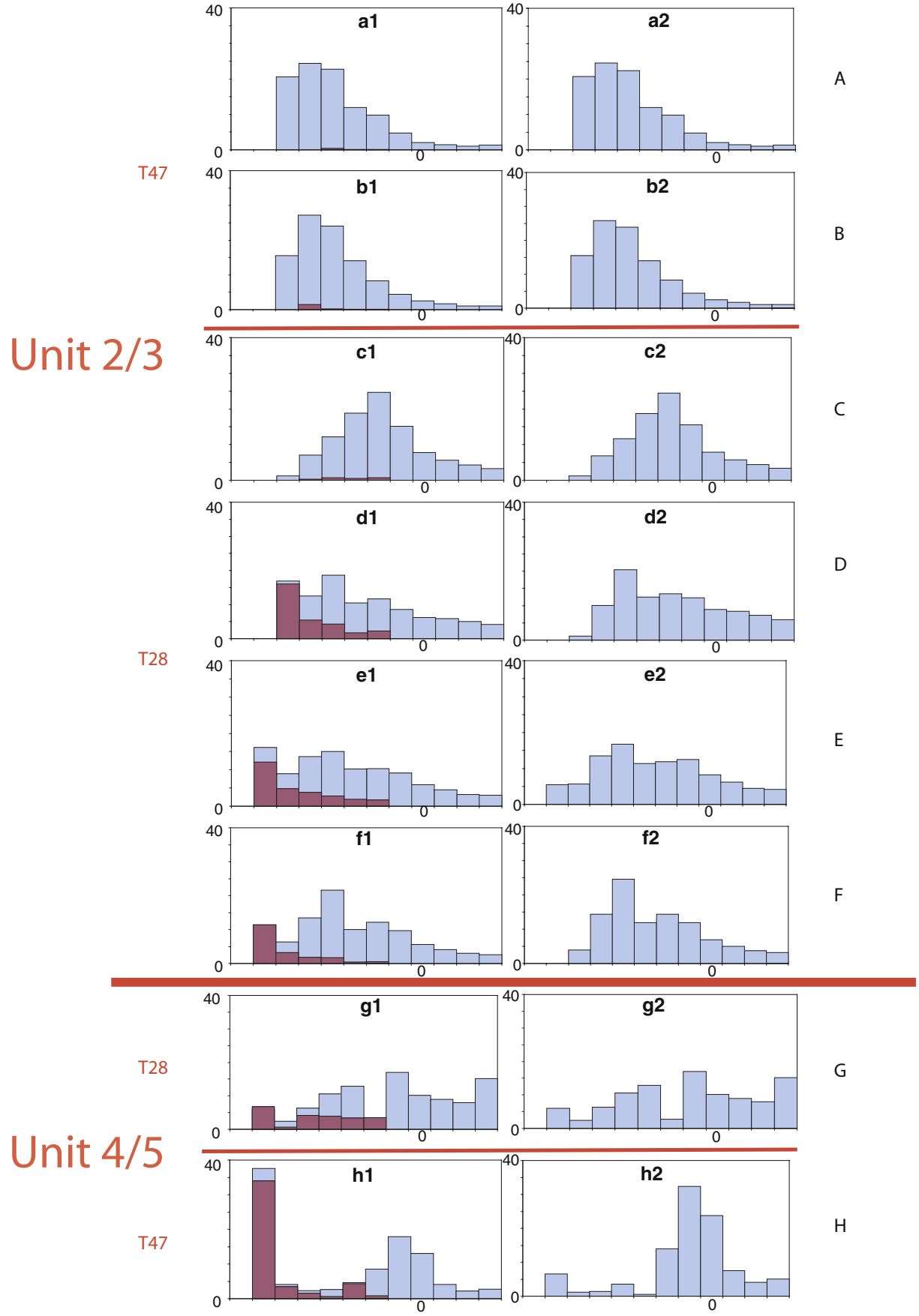
a1
a2
b1
b2
c1
c2
d1
d2
e1
e2
f1
f2
g1
g2
h1
h2
40
0
A
B
C
D
E
F
G
H
T47
T28
T28
T47
Unit 2/3
Unit 4/5

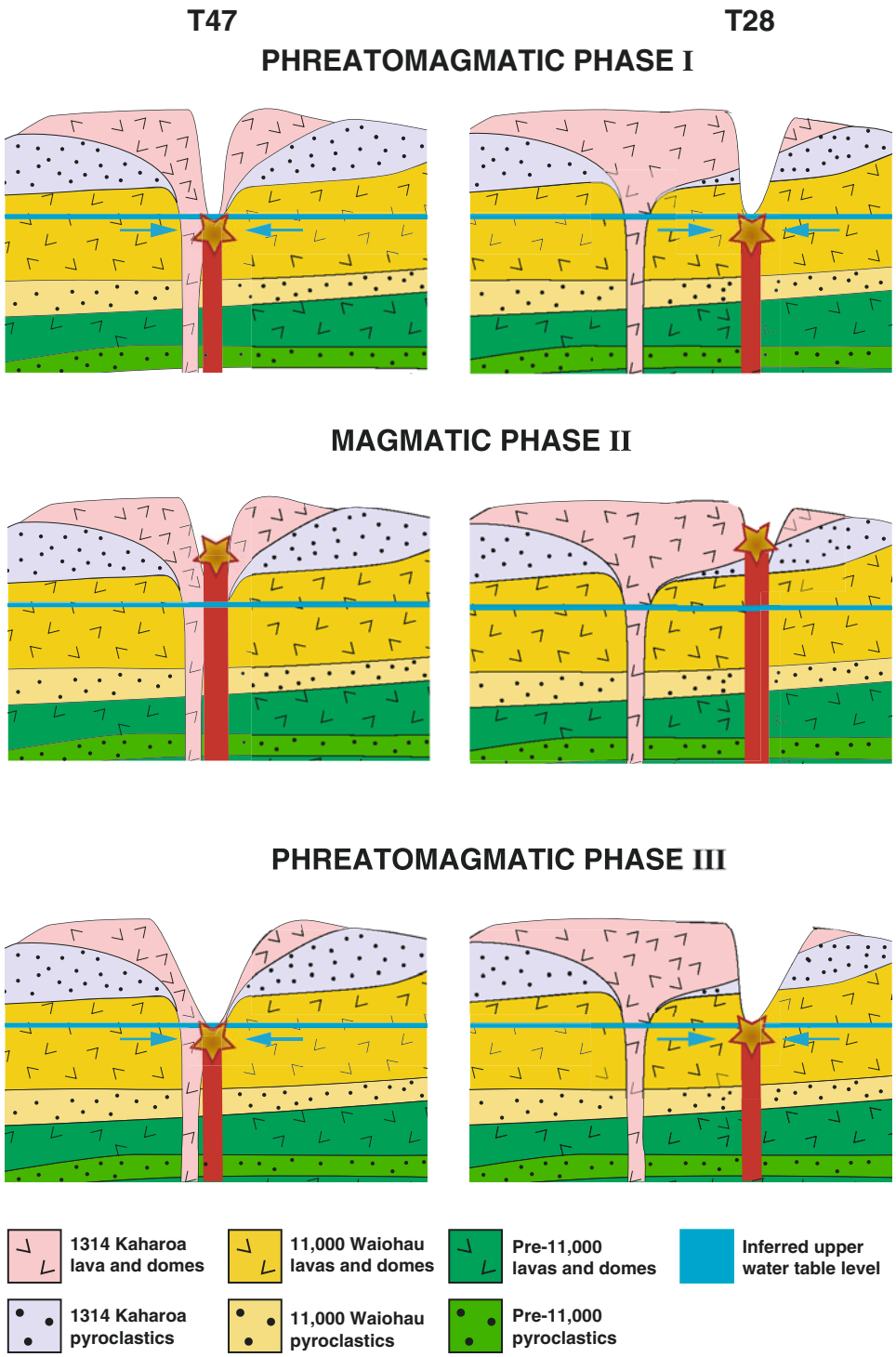

Fig. 15 Cartoon illustrating the fragmentation surface and interaction with groundwater at each section for phases I, II and III. In phase I, the fragmentation surface is within the water table resulting in phreatomagmatic activity at both sections. Throughout phase II, the fragmentation surface had risen above the water table resulting in largely magmatic explosive activity at both sections. In the crater adjacent to T47, the fragmentation surface was within stable and massive lavas, whereas at T28 the fragmentation surface was within both the 1314 A.D. Kaharoa pyroclastics and the dome margin. In the final phase III, magma withdrawal allowed the fragmentation surface to drop to levels once again below the water table resulting in phreatomagmatic activity and vent/conduit widening

transition into unit 4/5 (Fig. 10b). Pre-Kaharoa lithic clasts are almost absent in unit 2/3 at T47 (Fig. 12). In contrast, unit 2/3 deposits at T28 are characterized by a high and fluctuating wall rock lithic content (Fig. 10a).

In combination with independent evidence for water involvement, such as quenched, dense juvenile clasts, the abundance of wall-rock lithic clasts is often tagged as a measure of the extent of magma/water interaction, partic-

ularly if the water phase is in the form of groundwater. However, at Tarawera, the T28 unit 2/3 deposits, particularly the packages of weak dispersal, consist predominantly of moderately to highly vesicular juvenile clasts with ragged and fluidal morphologies yet commonly have high lithic contents (up to 42 wt%: Fig. 10a). Incorporation of wall rock particles can occur by a number of processes: explosive disruption of conduit walls adjacent to the fragmentation surface (Barberi et al. 1989; Suzuki-Kamata et al. 1993; Wilson and Hildreth 1997), incorporation of material that has collapsed or fallen from the walls of the vent and shallower conduit (Self et al. 1974) and sometimes the entrainment of loose wall rock by gas and pyroclasts above the fragmentation surface (Houghton and Nairn 1991). Wall rock content derived by explosive fragmentation of vent/conduit walls will increase with the intensity of the eruption and thus, generally, scoria/spatter cone-forming eruptions are lithic-poor (Fisher and Schmincke 1984; Cas and Wright 1987). This suggests that the high lithic contents at T28 reflect one of the other processes described above. Alternating lithic rich and poor beds, containing identical populations of highly vesicular ragged juvenile clasts at T28, are interpreted here to reflect passive incorporation of lithic clasts accompanying instability and collapse of the vent walls. This conclusion is consistent with observations at T28 that (with the exception of one bed) over 90% of all lithic clasts within each measured bed are derived from the shallow Kaharoa domes (Fig. 13b) coupled with the position of the vent on the steep (angle of rest) margin of Wahanga dome, where instability would be most likely. Kaharoa lithic clasts within beds at T47 however, are less abundant and uniformly dispersed and pre-Kaharoa clasts are more abundant (Fig. 13b). The fissure propagates through the middle of Ruawahia dome and adjacent to T47, the massive lavas comprising the vent walls were more stable than the steeply jointed lavas at T28 and hence, there was less chance for lithic clasts to fall into the vent. The less abundant lithic population at T47 was thus probably generated largely by explosive fragmentation, excavating vent and conduit walls.

There is a very strong link between sorting and relative abundance of wall rock lithic clasts in the unit 2/3 and 4/5 deposits, which we interpret to mean that the rhyolitic wall rock particles were not fragmented by explosions but have dimensions related to the joint spacing in the lavas. We suggest firstly, that the fissure crossing the outer margin of Wahanga dome adjacent to T28, has resulted in a steep and extremely fragile vent area easily accessible to failing dome material throughout phases II and III. Secondly, the fluctuations of shallow Kaharoa lithic content over short vertical intervals at T28 throughout phase II, is suggestive of episodic vent clearing following short-lived collapses that also contributed to the process of vent widening in phase III, at both T28 and T47.

Nature of the phreatomagmatic phases I and III

The opening and closing phreatomagmatic units 1 and 4/5 can be distinguished on the basis of both morphology and vesicularity of the juvenile clasts and the nature and abundance of the wall rock component. The basal unit 1 deposits contain a mixture of scoria and knobbly dense lapilli which changes to a more uniform population of ragged scoria in upper beds within the unit. At both sections, juvenile clasts have typically wide vesicularity ranges, between 31 and 72%, with modal vesicularities between 45 and 64% (Table 2 and Sable et al. (in preparation)). The broad range of clast vesicularities in unit 1 implies that vesiculation was halted at different points in the degassing history of the portion of melt ejected at any one instant in time probably due to magma/water interaction deep in the conduit (>300 m depth). A change to an increasingly narrow unimodal population of highly vesicular clasts suggests that with time, the majority of the melt was rising relatively rapidly and actively vesiculating at time of fragmentation. Volatile exsolution played an increasingly significant role in melt fragmentation, thus producing an essentially homogenous population of vesicular clasts (Sable et al. (in preparation)).

Wall rock lithic clasts are present throughout unit 1 in varying proportions. In particular, the abundance of pre-Kaharoa lithic clasts within unit 1 is greater than for following units. Pre-Kaharoa lithic clasts are most abundant within lowermost beds of unit 1 and show a continual decrease with time and stratigraphic height. We interpret this to mean that fragmentation began at relatively deep levels (>300 m) with access of groundwater, but then rapidly became shallower as the eruption proceeded and an increase of magma flux allowed the fragmentation surface to rise to levels above the water table by the close of phase I. Pre-Kaharoa lithic clasts are scarce to absent in unit 2/3 deposits at both sections and we infer that the fragmentation surface had risen to, and remained, above the level of the pre-Kaharoa deposits for most of this phase.

In contrast to unit 1, juvenile clasts within phreatomagmatic unit 4/5 have the largest vesicularity ranges of the entire eruption, with much lower mean values of 38–45% and often polymodal distributions (Table 2; Sable et al. (in preparation)). The wide ranges of observed vesicularities in part reflects recycling of previously erupted material, but may also be partly attributed to the slowing, stalling and ultimately retreat of portions of the magma within the vent and shallow conduit. Unit 4/5 also has the highest diversity of juvenile clast morphologies amongst the 1886 deposits, including kügel lapilli and dike wall fragments, and the population of larger clasts is dominated by flattened, degassed dense bombs with breadcrust textures. The vesicularity data, in combination with this diversity of

juvenile morphologies, suggests that fragmentation during phase 4/5 was due to a complex mixture of internal (vesiculation) and external (magma:water interaction) factors. The transition to unit 4/5 is inferred to be the result of lower magma supply rates and partial open-system degassing, resulting in a low efficiency of fragmentation and episodic explosions. The data suggest that during the waning stages of the eruption, magma in the conduit underwent partial open-system behavior and by the onset of phase III, this relatively degassed magma was reaching the surface at a reduced rate of ascent and, as a consequence, the fragmentation surface retreated down the conduit towards the water table. We suggest that this favored renewed magma/water interaction, reflected in the increasing abundance of poor to moderately vesicular juvenile clasts with quenched textures and rounded cauliflower morphologies. A significant subpopulation of pre-Kaharoa clasts (Fig. 12), are most abundant in the final beds, suggest that the fragmentation surface was lowered to a level where explosions were occurring within the deeper, i.e., ~>300 m pre-Kaharoa stratigraphy.

Nature of phase II

Interpretation of vesicularity data and implications for the history of phase II magma

Sable et al. (in preparation) have suggested a very similar history of deep magma ascent, vesiculation and fragmentation of the magma erupted at T28 and from the Plinian vents, like that adjacent to T47. Therefore we suggest that shallow seated controls possibly controlled the contrasting eruptive styles and intensities both between vents at T28 and T47 and along the whole length of the fissure. In particular the incorporation of variable amounts of cold lithic wall rock into the vent and shallow conduit via wall collapses must have had drastic effects on the dynamics and thermodynamics of the erupting jet.

Influence of wall rock incorporation on eruptive style

The section T28 deposits have high abundances of wall rock particles (up to 42 wt%) throughout unit 2/3. The grain size of the rhyolitic particles entering the vent and shallow conduit ranges over 12 phi units. The incorporation of this cold wall rock and pyroclastic material must dampen the jet phase of the eruption, with significant thermal and physical effects:

(a) The principal physical effect is related to a reduction of the velocity of the jet accompanying the increased mass. The physical loading of lithic particles initially at rest into the jet would lead to a dramatic reduction in speed. Application of a simple equation for conservation of momentum implies that the incorporation of 20–35 wt% of wall rock lithic particles would reduce the velocity of the jet to 70–80% of it's former value (Wilson, 2006, personal communication). This is probably a minimum value as it only allows for the lithic component of the material that is coarser than 4 mm.

(b) The incorporation of cold water-saturated wall rock has severe consequences for the thermal structure of the jet. The heat required to boil off any water has a dramatic effect by reducing the capacity for heating of the entrained air and hence stable eruption column development.

The jet phase adjacent to sites such as T28 therefore must have been much slower and more dense relative to that at the four principal Plinian vents, including that adjacent to T47 (Sable et al. 2006). A detailed quantitative model for the thermal influence of the incorporated wall rock will be the subject of the next phase of investigation.

Implications of accumulation rates

The very high proximal accumulation rates (9.5 m/h) for the widely dispersed packages, as seen at section T47, are due to sedimentation due to (1) clasts exiting from the margins of the jet and column; (2) ballistics; and (3) the high plume (Sable et al. 2006). At these four vents, the bulk of the erupted mass enters the convective and umbrella-cloud portions of the plume and is sedimented out in the medial and distal regions. The over-thickened proximal deposits at Tarawera have similar thinning rates to those observed in the proximal 1912 Novarupta Plinian fall deposits, the only other eruption where ultraproximal deposits have been studied in this detail. The high accumulation rates observed at these ultraproximal sites could be common for other Plinian eruptions that lack exposure within the ultraproximal region (e.g. caldera lakes).

The situation at the vents adjacent to T28, and other vents which produced packages with thickness half distance values of <50 m must have been somewhat different. Here it is clear that little or no mass from these vents entered the high plume. Instead the bulk of the erupted material was sedimented prematurely within 400 m of vent in cone-forming packages. The discharge rate was clearly lower than for the associated vents feeding the high plume but still very high with respect to classical fountaining eruptions styles. Accumulation rates of 5.1 m/h for the cone-forming parts of this deposit are more than an order of magnitude greater than those typical of Hawaiian and Strombolian eruptions, as described above. To a first order discharge rates from vents like T28 must have also been at least an order of magnitude higher. Average accumulation rates calculated for sub Plinian eruptions such as Paricutin (0.2 m/h), Ruapehu 1996 (0.31 m/h) and Tolbachik 1975

(0.4–0.6 m/h) (see Sable et al. 2006 for table of accumulation rates) are also an order of magnitude less than those observed at Tarawera. We suggest that vents like those adjacent to T28 would have contributed mass to the high Plinian plume but for the influence of vent wall instability at these sites. The relatively high degree of incorporation of cold wall rock and pyroclastics at T28, and like vents, led to heightened instabilities in the jet phase and premature sedimentation phasing the ultraproximal region.

Conclusions

Contrasts in eruptive style between phases

The 1886 eruption of Mt. Tarawera was a short-lived, yet sustained and highly explosive event with three distinct phases of contrasting eruption style. The initial products formed in a series of phreatomagmatic discrete explosions along the 8 km length of Mt Tarawera. Fragmentation probably began at depths of a few hundred meters beneath the newly forming fissure as ascending basaltic magma came into contact with water-bearing pre-Kaharoa and Kaharoa lavas and pyroclastics. The second, high intensity phase of the eruption generated coarse scoria cones along the fissure synchronously with the widespread Plinian fall deposit. This phase varied in intensity and dispersal throughout its duration and at different points along the 8 km length of the northeastern fissure. The fragmentation surface had risen to within the near-surface Kaharoa deposits for the entire northeastern fissure segment for most of the second phase. This is an interesting conclusion given that the majority of the widespread scoria fall occurred during this phase, implying that fragmentation driving the intense Plinian phase of the eruption was at a very shallow level (i.e. generally no more that 200–300 m below the modern surface). At the close of phase II, the magma in the conduit became progressively depleted in volatiles due to the onset of partial open-system behavior. The third phase generated the unit 4/5 deposits, with limited magma/water interaction. The high wall rock contents of unit 4/5 and the abundance of pre-Kaharoa rhyolite suggest that the fragmentation surface lowered to depths greater than 300 m, accompanying magma withdrawal in the final stages of the eruption.

Contrasting eruptive processes during phase II along the 1886 fissure

In comparison to phases I and III, phase II was variable in eruptive style and intensity. At T28, rapid and abrupt shifts in grain size suggests a non-sustained or fluctuating eruption style, induced by large-scale collapses of vent walls. At T47 we infer a stronger role for more intense, sustained eruptive conditions, not interrupted by major wall-rock collapses. Sable et al. (2006) suggest that low fountaining activity of varying intensity was dominant during phase II at T28, and that ejecta from this style of activity mixed with only minor amounts of material produced from the Plinian plume from other portions of the fissure system. In contrast, T47 was adjacent to at least one major Plinian source (Crater I) of pyroclasts entering the high intensity plume producing the widespread scoria fall (Sable et al. 2006). The resulting mixed assemblages of clasts reflect material falling from the full height of the plume together with clasts from the margin of the jet and from adjacent low fountains. This strong contrast in style and intensity of the eruptions producing the proximal unit 2/3 deposits is strongly reflected in diversity of thinning half distances and is only weakly reflected in the grain size characteristics of the deposits. This lack of major contrast in grain size between packages of widespread and local dispersal reflects (1) similarity of fragmentation processes at all vents; (2) the insensitivity of grain size to shifts in eruptive intensity (as opposed to say major changes of magma/water ratio); and (3) the fact that the clast population in any bed reflects mixing of material erupted from adjacent vents of contrasting eruptive intensity. Packages of widespread and local dispersal however, have significant componentry contrasts. Locally dispersed packages are richer in shallow Kaharoa lithic clasts and more widespread packages are dominated by vesicular juvenile scoria (Fig. 8a, b).

Influences of the incorporated wall rock on the jet phase

The 1886 deposits demonstrate that under certain conditions eruptive style and intensity can be strongly influenced by processes originating in the very shallow (<200 m) conduit. Instability of the shallow conduit/vent walls led to incorporation of high but variable amounts of cold, rhyolitic wall rock into the emergent jet phase along some segments of the north eastern fissure. This incorporation clearly had major physical and perhaps thermal consequences for the structure of the jet and led to early sedimentation of significant volumes of ejecta at high accumulation rates, which were confined to within 400 m of vent thus corresponding to less intense activity with respect to adjacent Plinian vents.

Implications for other Plinian eruptions

Overthickened proximal cone-forming deposits have been documented from Plinian eruptions (Novarupta, Quizapu). Cone-forming deposits at Tarawera have similar thinning rates to those observed in the proximal 1912 Novarupta deposits but, however, higher accumulation rates. Are there unusual circumstances that apply to the 1886 eruption and

led to the formation of the cone forming proximal deposits? For example, was it critical that this was a fissure fed eruption or was the key that the vent/conduit walls were unusually unstable? The alternative is simply that proximal exposure of this quality is extremely rare for even historical Plinian eruptions and perhaps proximal sedimentation of this kind is more common than the literature would imply.

Acknowledgements We acknowledge financial support from NSF (EAR-01-25719 and EAR-05-37459) and the New Zealand Foundation for Research, Science & Technology. We thank Judy, Fleur and Steve Collins for access to the mountain and helicopter logistic support. Michael Rosenberg was a willing and cheerful companion during field work on Tarawera. The manuscript benefited greatly from constructive comments from Raffaello Cioni and two anonymous reviewers.

References

Barberi F, Cioni R, Rosi M, Santacroce R, Sbrana A, Vecci R (1989) Magmatic and phreatomagmatic phases in explosive eruptions of Vesuvius as deduced by grain-size and component analysis of the pyroclastic deposits. J Volcanol Geotherm Res 38:287–307

Cas RAF, Wright JV (1987) Volcanic successions: modern and ancient. Allen, London, p 528

Cole JW (1970) Structure and eruptive history of the Tarawera Volcanic Complex. NZ J Geol Geophys 13:879–902

Coltelli M, Del Carlo P, Vezzoli L (1995) A Plinian eruption of basaltic composition in the historical activity of Mt. Etna. Per Mineral 64:145–146

Fisher RV, Schmincke HU (1984) Pyroclastic rocks. Springer, Berlin Heidelberg New York, p 472

Houghton BF, Hackett WR (1984) Strombolian and phreatomagmatic deposits of Ohakune craters, Ruapehu, New Zealand: a complex interaction between external water and rising basaltic magma. J Volcanol Geotherm Res 21:207–231

Houghton BF, Nairn IA (1991) The 1976–1982 Strombolian and phreatomagmatic eruptions of White Island, New Zealand: eruptive and depositional mechanisms at a 'wet' volcano. Bull Volcanol 54:25–49

Houghton BF, Schmincke H-U (1989) Rothenberg scoria cone, East Eifel: a complex strombolian and phreatomagmatic volcano. Bull Volcanol 52:28–48

Houghton BF, Wilson CJN (1998) Fire and water: physical roles of water in large eruptions at Taupo and Okataina calderas. In: Arehart GB, Hulston JR (eds) Water-rock interaction. Proc 9th Int Symp Water-Rock Interaction, Taupo, New Zealand, 30 March–3 April 1998. AA Balkema, Rotterdam, pp 25–30

Houghton BF, Wilson CJN, McWilliams MO, Lanphere MA, Weaver SD, Briggs RM, Pringle MS (1995) Chronology and dynamics of a large silicic magmatic system: central Taupo Volcanic Zone, New Zealand. Geology 23:13–16

Houghton BF, Wilson CJN, Smith IEM (1999) Shallow-seated controls on styles of explosive basaltic volcanism: a case study from New Zealand. J Volcanol Geotherm Res 91:97–120

Houghton BF, Bonadonna C, Gregg CE, Johnston DM, Cousins WJ, Cole JW, Del Carlo P (2006) Proximal tephra hazards: recent eruption studies applied to volcanic risk in the Auckland volcanic field, New Zealand. J Volcanol Geothermal Res 155:138–149

Jaupart C (1996) Physical models of volcanic eruptions. Chem Geol 128:217–227

Keam RF (1988) Tarawera: the volcanic eruption of 10 June 1886, Auckland, New Zealand, p 472 (Published by the author)

Leonard GS, Self S, Cole JW, Nairn IA (2002) Basalt triggering of the c. A.D. 1305 Kaharoa rhyolite eruption, Tarawera Volcanic Complex, New Zealand. J Volcanol Geotherm Res 115:461–486

Nairn IA (1979) Rotomahana-Waimangu eruption, 1886: base surge and basalt magma. NZ J Geol Geophys 22:363–378

Nairn IA (2002) Geology of the Okataina Volcanic Centre, scale 1:50,000. Institute of Geological & Nuclear Sciences geological map 25. 1 sheet + 156 p. Institute of Geological & Nuclear Sciences Limited, Lower Hutt, New Zealand

Nairn IA, Cole JW (1981) Basalt dikes in the 1886 Tarawera Rift. NZ J Geol Geophys 24:585–592

Nairn IA, Scutter C, Self S, Cole JW, Leonard GS (2001) Distribution, stratigraphy, and history of proximal deposits from the c. A.D. 1305 Kaharoa eruptive episode at Tarawera Volcano, New Zealand. NZ J Geol Geophys 44:467–484

Parfitt EA, Wilson L (1995) Explosive volcanic eruptions-IX. The transition between Hawaiian-style lava fountaining and Strombolian explosive activity. Geophys J Int 121:226–232

Pyle DM (1989) The thickness, volume and grainsize of tephra fall deposits. Bull Volcanol 51:1–15

Sable JE, Houghton BF, Wilson CJN, Carey RJ (2006) Complex proximal sedimentation from Plinian plumes: the example of Tarawera 1886. Bull Volcanol 69:89–103

Self S, Sparks RSJ, Booth B, Walker GPL (1974) The 1973 Heimaey strombolian scoria deposit, Iceland. Geol Mag 111:539–548

Simmons SF, Keywood M, Scott BJ, Keam RF (1993) Irreversible change of the Rotomahana-Waimangu hydrothermal system (New Zealand) as a consequence of a volcanic eruption. Geology 21:643–646

Smith SP (1886a) The eruption of Tarawera: a report to the Surveyor General. Government Printer, Wellington, New Zealand

Smith SP (1886b) Preliminary report on the volcanic eruption at Tarawera. J House Represent Commonw, New Zealand H-26:1–4

Suzuki-Kamata K, Kamata H, Bacon CR (1993) Evolution of the caldera-forming eruption at Crater Lake, Oregon, indicated by component analysis of lithic fragments. J Geophys Res 98:14059–14074

Thomas APW (1888) Report on the eruption of Tarawera and Rotomahana. Government Printer, Wellington, New Zealand

Walker GPL (1973) Explosive volcanic eruptions-a new classification scheme. Geol Rundsch 62:431–446

Walker GPL, Croasdale R (1972) Characteristics of some basaltic pyroclastics. Bull Volcanol 35:303–317

Walker GPL, Self S, Wilson L (1984) Tarawera 1886, New Zealand-a basaltic Plinian fissure eruption. J Volcanol Geotherm Res 21:61–78

Williams WL (1887) Phenomena connected with the Tarawera eruption of 10th of June as observed at Gisborne. Trans NZ Inst 19:380–382

Williams SN (1983) Plinian airfall deposits of basaltic composition. Geology 11:211–214

Wilson L, Head JW (1981) Ascent and eruption of basaltic magma on the Earth and Moon. J Geophys Res 86:2971–3001

Wilson CJN, Hildreth W (1997) The Bishop Tuff: new insights from eruptive stratigraphy. J Geol 105:407–439

Wilson CJN, Houghton BF, McWilliams MO, Lanphere MA, Weaver SD, Briggs RM (1995) Volcanic and structural evolution of Taupo Volcanic Zone, New Zealand: a review. J Volcanol Geotherm Res 68:1–28